

# Doppler Spread Estimation in MIMO Frequency-selective Fading Channels

Mostafa Mohammadkarimi, *Student Member, IEEE*, Ebrahim Karami, *Student Member, IEEE*, Octavia A. Dobre, *Senior Member, IEEE*, and Moe Z. Win *Fellow, IEEE*

## Abstract

One of the main challenges in high-speed mobile communications is the presence of large Doppler spreads. Thus, accurate estimation of maximum Doppler spread (MDS) plays an important role in improving the performance of the communication link. In this paper, we derive the data-aided (DA) and non-data-aided (NDA) Cramer-Rao lower bounds (CRLBs) and maximum likelihood estimators (MLEs) for the MDS in multiple-input multiple-output (MIMO) frequency-selective fading channel. Moreover, a low-complexity NDA-moment-based estimator (MBE) is proposed. The proposed NDA-MBE relies on the second- and fourth-order moments of the received signal, which are employed to estimate the normalized squared autocorrelation function of the fading channel. Then, the problem of MDS estimation is formulated as a non-linear regression problem, and the least-squares curve-fitting optimization technique is applied to determine the estimate of the MDS. This is the first time in the literature when DA- and NDA-MDS estimation is investigated for MIMO frequency-selective fading channel. Simulation results show that there is no significant performance gap between the derived NDA-MLE and NDA-CRLB even when the observation window is relatively small. Furthermore, the significant reduced-complexity in the NDA-MBE leads to low root-mean-square error (NRMSE) over a wide range of MDSs when the observation window is selected large enough.

## Index Terms

Maximum Doppler spread, data-aided, non-data-aided, multiple-input multiple-output, frequency-selective, Cramer-Rao lower bound (CRLB), fourth-order moment, autocorrelation, non-linear regression, maximum likelihood estimator (MLE).

## I. INTRODUCTION

**M**AXIMUM DOPPLER SPREAD measures the coherence time, related to the rate of change, of wireless communication channels. Its knowledge is important to design efficient wireless communication systems for high-speed vehicles [1]–[3]. In particular, accurate estimation of the maximum Doppler spread (MDS) is required for the design of adaptive transceivers, as well as in cellular and smart antenna systems [3]–[12]. For example, in the context of adaptive transceivers, system parameters such as coding, modulation, and power are adapted to the changes in the channel [4]–[7]. In cellular systems, handoff is dictated by the velocity of the mobile station, which is also directly obtained from the Doppler information. Knowledge of the rate of the channel change is also employed to reduce unnecessary handoff; the handoff is initiated based on the received power at the mobile station, and the optimum window size for power estimation depends on the MDS [7]–[10]. In the context of smart antenna systems, the MDS is used in the design of the maximum likelihood (ML)

M. Mohammadkarimi, E. Karami, and O. A. Dobre are with the Department of Electrical and Computer Engineering, Memorial University, St. John's, NL, Canada (e-mail: {m.mohammadkarimi, ekarami, odobre}@mun.ca).

M. Z. Win is with the Laboratory for Information and Decision Systems (LIDS), Massachusetts Institute of Technology, Cambridge, MA, USA (e-mail: moewin@mit.edu).

space-time transceivers [11], [12]. In addition, knowledge of MDS is required for channel tracking and equalization, as well as for the selection of the optimal interleaving length in wireless communication systems [13].

In general, parameter estimators can be categorized as: i) data-aided (DA), where the estimation relies on a pilot or preamble sequence [14]–[18], ii) non-data-aided (NDA), where the estimation is performed with no *a priori* knowledge about the transmitted symbols [19]–[23], and iii) code-aided (CA), where the decoding gain is used via iterative feedback to enhance the estimation performance of the desired parameters [24]–[29].

With regard to the MDS estimation, the DA approach often provides accurate estimates for slowly-varying channels by employing a reduced number of pilot symbols, whereas this does not hold for fast-varying channels. In the latter case, the details of the channel variations cannot be captured accurately, and more pilots are required, which results in increased overhead and reduced system capacity.

There are five major classes of MDS estimators: ML-based, power spectral density (PSD)-based, level-crossing-rate (LCR)-based, covariance-based, and cyclostationarity-based estimators. The ML-based estimator maximizes the likelihood function, and, in general, is asymptotically unbiased, achieving the Cramer-Rao lower bound (CRLB) [30]–[32]. However, maximum likelihood estimator (MLE) for MDS suffers from significant computational complexity. Hence, different modified low-complexity MLEs for MDS in single-input single-output (SISO) flat-fading channel were developed [33], [34]. With the PSD-based estimators, some unique features from the Doppler spectrum are obtained through the sample periodogram of the received signal [35]. Covariance-based estimators extract the Doppler information which exists in the sample auto-covariance of the received signal [36]–[38]. LCR-based estimators rely on the number of level crossings of the received signal statistics, which is proportional to the MDS [39]. The cyclostationarity-based estimators exploit the cyclostationarity of the received signal [40]. Comparing with other MDS estimators, the advantage of the cyclostationarity-based estimators is the robustness to stationary noise and interference.

While the problem of MDS estimation in SISO flat-fading channel has been extensively investigated in the literature [30]–[40], the MDS estimation in multiple-input multiple-output (MIMO) frequency-selective or in MIMO flat-fading channel has not been considerably explored. Furthermore, DA-MDS estimation has mainly been studied in the literature. To the best of our knowledge, only a few works have addressed MDS estimation in conjunction with multiple antenna systems. In [32], the authors derived an asymptotic DA-MLE and DA-CRLB for joint MDS and noise variance estimation in MIMO flat-fading channel. In [40], the cyclic correlation (CC) of linearly modulated signals is exploited for the MDS estimation for single transmit antenna scenarios. While both DA and NDA estimators are studied in [40], only frequency-flat fading and single transmit antenna are considered.

In this paper, we investigate the problem of MDS estimation in MIMO frequency-selective fading channel for both DA and NDA scenarios. The DA-CRLB, NDA-CRLB, DA-MLE, and NDA-MLE in MIMO frequency-selective fading channel are derived. In addition, a low-complexity NDA-moment-based estimator (MBE) is proposed. The proposed MBE relies on the second- and fourth-order moments of the received signal along with the least-square (LS) curve-fitting optimization technique to estimate the normalized squared autocorrelation function (AF) and MDS of the fading channel. Since the proposed MBE is NDA, it removes the need of pilots and preambles used for DA-MDS estimation, and thus, it results in increased system

capacity. The NDA-MBE outperforms the derived DA-MLE in the presence of imperfect time-frequency synchronization. Also, the MBE outperforms the NDA-CC estimator (CCE) in [40] and the DA low-complexity MLE in [33], [34] in SISO systems and under flat fading channels and in the presence of perfect time-frequency synchronization.

### A. Contributions

This paper brings the following original contributions:

- The DA- and NDA-CRLBs for MDS estimation in MIMO frequency-selective fading channel are derived;
- The DA- and NDA-MLEs for MDS in MIMO frequency-selective fading channel are derived;
- A low-complexity NDA-MBE is proposed. The proposed estimator exhibits the following advantages:
  - lower computational complexity compared to the MLEs;
  - does not require time synchronization;
  - is robust to the carrier frequency offset;
  - increases system capacity;
  - does not require *a priori* knowledge of noise power, signal power, and channel delay profile;
  - does not require *a priori* knowledge of the number of transmit antennas;
  - removes the need of joint parameter estimation, such as carrier frequency offset, signal power, noise power, and channel delay profile estimation;
- The optimal combining method for the NDA-MBE in case of multiple receive antennas is derived through the bootstrap technique.

### B. Notations

*Notation.* Random variables are displayed in sans serif, upright fonts; their realizations in serif, italic fonts. Vectors and matrices are denoted by bold lowercase and uppercase letters, respectively. For example, a random variable and its realization are denoted by  $x$  and  $x$ ; a random vector and its realization are denoted by  $\mathbf{x}$  and  $\mathbf{x}$ ; a random matrix and its realization are denoted by  $\mathbf{X}$  and  $\mathbf{X}$ , respectively. Throughout the paper,  $(\cdot)^*$  is used for the complex conjugate,  $(\cdot)^\dagger$  is used for transpose,  $|\cdot|$  represents the absolute value operator,  $\lfloor \cdot \rfloor$  is the floor function,  $\delta_{i,j}$  denotes the Kronecker delta function,  $n!$  is the factorial of  $n$ ,  $\mathbb{E}\{\cdot\}$  is the statistical expectation,  $\hat{x}$  is an estimate of  $x$ , and  $\det(\mathbf{A})$  denotes the determinant of the matrix  $\mathbf{A}$ .

The rest of the paper is organized as follows: Section II describes the system model; Section III obtains the DA- and NDA-CRLBs for MDS estimation in MIMO frequency-selective fading; Section IV derives the DA- and NDA-MLEs for MDS in MIMO frequency-selective fading channel; Section V introduces the proposed NDA-MBE for MDS; Section VI evaluates the computational complexity of the derived estimators; Section VII presents numerical results; and Section VIII concludes the paper.

## II. SYSTEM MODEL

Let us consider a MIMO wireless communication system with  $n_t$  transmit antennas and  $n_r$  receive antennas, where the received signals are affected by time-varying frequency-selective Rayleigh fading and are corrupted by additive white Gaussian noise. The discrete-time complex-valued baseband signal at the  $n$ th receive antenna is expressed as [41]

$$r_k^{(n)} = \sum_{m=1}^{n_t} \sum_{l=1}^L h_{k,l}^{(mn)} s_{k-l}^{(m)} + w_k^{(n)} \quad k = 1, \dots, N, \quad (1)$$

where  $N$  is the number of observation symbols,  $L$  is the length of the channel impulse response,  $s_k^{(m)}$  is the symbol transmitted from the  $m$ th antenna at time  $k$ , satisfying  $\mathbb{E}\{s_{k_1}^{(m_1)}(s_{k_2}^{(m_2)})^*\} = \sigma_{s_{m_1}}^2 \delta_{m_1, m_2} \delta_{k_1, k_2}$ , with  $\sigma_{s_{m_1}}^2$  being the transmit power of the  $m_1$ th antenna,  $w_k^{(n)}$  is the complex-valued additive white Gaussian noise at the  $n$ th receive antenna at time  $k$ , whose variance is  $\sigma_{w_n}^2$ , and  $h_{k,l}^{(mn)}$  denotes the zero-mean complex-valued Gaussian fading process between the  $m$ th transmit and  $n$ th receive antennas for the  $l$ th tap of the fading channel and at time  $k$ . It is considered that the channels for different antennas are independent, with the cross-correlation of the  $l_1$  and  $l_2$  taps given by<sup>1</sup>

$$\mathbb{E}\{h_{k,l_1}^{(mn)}(h_{k+u,l_2}^{(mn)})^*\} = \sigma_{h_{(mn),l_1}}^2 J_0(2\pi f_D T_s u) \delta_{l_1, l_2}, \quad (2)$$

where  $J_0(\cdot)$  is the zero-order Bessel function of the first kind,  $\sigma_{h_{(mn),l_1}}^2$  is the variance of the  $l_1$ th tap between the  $m$ th transmit and  $n$ th receive antennas,  $T_s$  denotes the symbol period, and  $f_D = v/\lambda = f_c v/c$  represents the MDS in Hz, with  $v$  as the relative speed between the transmitter and receiver,  $\lambda$  as the wavelength,  $f_c$  as the carrier frequency, and  $c$  as the speed of light.

## III. CRLB FOR MDS ESTIMATION

In this section, the DA- and NDA-CRLB for MDS estimation in MIMO frequency-selective fading channel are derived.

### A. DA-CRLB

Let us consider  $s_k^{(m)} = s_k^{(m)}$ ,  $m = 1, 2, \dots, n_t$ ,  $k = 1, 2, \dots, N - L + 1$ , as employed pilots for DA-MDS estimation. The received signal at  $n$ th receive antenna in (1) can be written as

$$\begin{aligned} r_k^{(n)} &= \bar{r}_k^{(n)} + j\check{r}_k^{(n)} = \sum_{m=1}^{n_t} \sum_{l=1}^L \bar{h}_{k,l}^{(mn)} \bar{s}_{k-l}^{(m)} - \check{h}_{k,l}^{(mn)} \check{s}_{k-l}^{(m)} + \bar{w}_k^{(n)} \\ &\quad + j \left( \sum_{m=1}^{n_t} \sum_{l=1}^L \bar{h}_{k,l}^{(mn)} \check{s}_{k-l}^{(m)} + \check{h}_{k,l}^{(mn)} \bar{s}_{k-l}^{(m)} + \check{w}_k^{(n)} \right), \end{aligned} \quad (3)$$

where  $\bar{r}_k^{(n)} \triangleq \text{Re}\{r_k^{(n)}\}$ ,  $\check{r}_k^{(n)} \triangleq \text{Im}\{r_k^{(n)}\}$ ,  $\bar{h}_{k,l}^{(mn)} \triangleq \text{Re}\{h_{k,l}^{(mn)}\}$ ,  $\check{h}_{k,l}^{(mn)} \triangleq \text{Im}\{h_{k,l}^{(mn)}\}$ ,  $\bar{s}_{k-l}^{(m)} \triangleq \text{Re}\{s_{k-l}^{(m)}\}$ , and  $\check{s}_{k-l}^{(m)} \triangleq \text{Im}\{s_{k-l}^{(m)}\}$ .

Let us define

$$\mathbf{r}^{(n)} \triangleq \left[ \bar{r}_1^{(n)} \ \bar{r}_2^{(n)} \ \dots \ \bar{r}_N^{(n)} \ \check{r}_1^{(n)} \ \check{r}_2^{(n)} \ \dots \ \check{r}_N^{(n)} \right]^\dagger \quad (4)$$

<sup>1</sup>Here we consider the Jakes channel; it is worth noting that different parametric channel models can be also considered.

and

$$\mathbf{r} \triangleq [\mathbf{r}^{(1)\dagger} \mathbf{r}^{(2)\dagger} \dots \mathbf{r}^{(n_r)\dagger}]^\dagger. \quad (5)$$

The elements of the vector  $\mathbf{r}^{(n)}$ ,  $n = 1, 2, \dots, n_t$ , are linear combinations of the correlated Gaussian random variables as in (3). Thus,  $\mathbf{r}$ , is a Gaussian random vector with probability density function (PDF) given by

$$p(\mathbf{r}|\mathbf{s}; \boldsymbol{\theta}) = \frac{\exp\left(-\frac{1}{2}\mathbf{r}^\dagger \boldsymbol{\Sigma}^{-1}(\mathbf{s}, \boldsymbol{\theta})\mathbf{r}\right)}{(2\pi)^{Nn_r} \det^{\frac{1}{2}}(\boldsymbol{\Sigma}(\mathbf{s}, \boldsymbol{\theta}))}, \quad (6)$$

where  $\boldsymbol{\Sigma}(\mathbf{s}, \boldsymbol{\theta}) \triangleq \mathbb{E}\{\mathbf{r}\mathbf{r}^\dagger\}$ ,  $\mathbf{s} \triangleq [\mathbf{s}^{(1)\dagger} \mathbf{s}^{(2)\dagger} \dots \mathbf{s}^{(n_t)\dagger}]^\dagger$ ,  $\mathbf{s}^{(m)} \triangleq [\bar{s}_1^{(m)} \bar{s}_2^{(m)} \dots \bar{s}_{N-L+1}^{(m)} \check{s}_1^{(m)} \check{s}_2^{(m)} \dots \check{s}_{N-L+1}^{(m)}]^\dagger$ , and  $\boldsymbol{\theta} \triangleq [\boldsymbol{\xi} \boldsymbol{\vartheta} f_D]^\dagger$  is the parameter vector, with

$$\boldsymbol{\xi} \triangleq [\sigma_{w_1}^2 \dots \sigma_{w_{n_r}}^2]^\dagger \quad (7a)$$

$$\boldsymbol{\vartheta} \triangleq [\boldsymbol{\vartheta}_1^\dagger \boldsymbol{\vartheta}_2^\dagger \dots \boldsymbol{\vartheta}_L^\dagger]^\dagger \quad (7b)$$

$$\boldsymbol{\vartheta}_l \triangleq \left[ \sigma_{h_{(11),l}}^2 \dots \sigma_{h_{(1n_r),l}}^2 \sigma_{h_{(21),l}}^2 \dots \sigma_{h_{(2n_r),l}}^2 \dots \sigma_{h_{(n_t 1),l}}^2 \dots \sigma_{h_{(n_t n_r),l}}^2 \right]^\dagger. \quad (7c)$$

Since  $\mathbf{r}^{(n_1)}$  and  $\mathbf{r}^{(n_2)}$ ,  $n_1 \neq n_2$ , are uncorrelated random vectors, i.e.  $\mathbb{E}\{\mathbf{r}^{(n_1)}\mathbf{r}^{(n_2)\dagger}\} = \mathbf{0}$ , the covariance matrix of  $\mathbf{r}$ ,  $\boldsymbol{\Sigma}(\mathbf{s}, \boldsymbol{\theta})$ , is block diagonal as

$$\boldsymbol{\Sigma}(\mathbf{s}, \boldsymbol{\theta}) \triangleq \mathbb{E}\{\mathbf{r}\mathbf{r}^\dagger\} = \begin{bmatrix} \boldsymbol{\Sigma}^{(1)} & & & \\ & \boldsymbol{\Sigma}^{(2)} & & \\ & & \ddots & \\ & & & \boldsymbol{\Sigma}^{(n_r)} \end{bmatrix}, \quad (8)$$

where  $\boldsymbol{\Sigma}^{(n)} \triangleq \mathbb{E}\{\mathbf{r}^{(n)}\mathbf{r}^{(n)\dagger}\}$ . By employing (2), (3), and (4), using the fact the real and imaginary part of the fading tap are independent random variables with  $\mathbb{E}\{|\bar{h}_{k,l}^{(mn)}|^2\} = \mathbb{E}\{|\check{h}_{k,l}^{(mn)}|^2\} = \sigma_{h_{(mn),l}}^2/2$ , and after some algebra, the elements of the covariance matrix  $\boldsymbol{\Sigma}^{(n)}$ ,  $n \in \{1, 2, \dots, n_r\}$ , are obtained as

$$\begin{aligned} \mathbb{E}\{\bar{r}_k^{(n)}\bar{r}_{k+u}^{(n)}\} &= \mathbb{E}\{\check{r}_k^{(n)}\check{r}_{k+u}^{(n)}\} \\ &= \frac{1}{2} \sum_{m=1}^{n_t} \sum_{l=1}^L \sigma_{h_{(mn),l}}^2 \left( \bar{s}_{k-l}^{(m)}\bar{s}_{k+u-l}^{(m)} + \check{s}_{k-l}^{(m)}\check{s}_{k+u-l}^{(m)} \right) \\ &\quad J_0(2\pi f_D T_s u) + \frac{\sigma_{w_n}^2}{2} \delta_{u,0} \end{aligned} \quad (9a)$$

$$\begin{aligned} \mathbb{E}\{\bar{r}_k^{(n)}\check{r}_{k+u}^{(n)}\} &= -\mathbb{E}\{\check{r}_k^{(n)}\bar{r}_{k+u}^{(n)}\} \\ &= \frac{1}{2} \sum_{m=1}^{n_t} \sum_{l=1}^L \sigma_{h_{(mn),l}}^2 \left( \bar{s}_{k-l}^{(m)}\check{s}_{k+u-l}^{(m)} - \check{s}_{k-l}^{(m)}\bar{s}_{k+u-l}^{(m)} \right) \end{aligned} \quad (9b)$$

$$J_0(2\pi f_D T_s u).$$

The Fisher information matrix of the parameter vector  $\boldsymbol{\theta}$ ,  $\mathbf{I}(\boldsymbol{\theta})$ , for the zero-mean Gaussian observation vector in (6) is obtained as

$$\begin{aligned} [\mathbf{I}(\boldsymbol{\theta})]_{ij} &\triangleq -\mathbb{E}\left\{\frac{\partial^2 \ln p(\mathbf{r}|\mathbf{s}; \boldsymbol{\theta})}{\partial \theta_i \partial \theta_j}\right\} \\ &= \frac{1}{2} \text{tr} \left[ \boldsymbol{\Sigma}^{-1}(\mathbf{s}, \boldsymbol{\theta}) \frac{\partial \boldsymbol{\Sigma}(\mathbf{s}, \boldsymbol{\theta})}{\partial \theta_i} \boldsymbol{\Sigma}^{-1}(\mathbf{s}, \boldsymbol{\theta}) \frac{\partial \boldsymbol{\Sigma}(\mathbf{s}, \boldsymbol{\theta})}{\partial \theta_j} \right]. \end{aligned} \quad (10)$$

For the MDS,  $f_D$ ,  $I(f_D) \triangleq [\mathbf{I}(\boldsymbol{\theta})]_{xx}$ ,  $x = n_t n_r L + n_r + 1$ , and one obtains

$$\begin{aligned} I(f_D) &= -\mathbb{E}\left\{\frac{\partial^2 \ln p(\mathbf{r}|\mathbf{s}; \boldsymbol{\theta})}{\partial f_D^2}\right\} \\ &= \frac{1}{2} \text{tr} \left[ \left( \boldsymbol{\Sigma}^{-1}(\mathbf{s}, \boldsymbol{\theta}) \frac{\partial \boldsymbol{\Sigma}(\mathbf{s}, \boldsymbol{\theta})}{\partial f_D} \right)^2 \right], \end{aligned} \quad (11)$$

where  $\frac{\partial \boldsymbol{\Sigma}(\mathbf{s}, \boldsymbol{\theta})}{\partial f_D}$  is obtained by replacing  $J_0(2\pi f_D T_s u)$  with  $-2\pi u T_s J_1(2\pi f_D T_s u)$  in  $\boldsymbol{\Sigma}(\mathbf{s}, \boldsymbol{\theta})$ , where  $J_1(\cdot)$  is the Bessel function of the first kind.

Finally, by employing (11), the DA-CRLB for MDS estimation in MIMO frequency-selective fading channel is obtained as

$$\text{Var}(\hat{f}_D) \geq I^{-1}(f_D) = \frac{1}{\frac{1}{2} \text{tr} \left[ \left( \boldsymbol{\Sigma}^{-1}(\mathbf{s}, \boldsymbol{\theta}) \frac{\partial \boldsymbol{\Sigma}(\mathbf{s}, \boldsymbol{\theta})}{\partial f_D} \right)^2 \right]}. \quad (12)$$

$$I(f_D) = -\mathbb{E}\left\{\frac{\partial^2 \ln p(\mathbf{r}; \boldsymbol{\varphi})}{\partial f_D^2}\right\} = -\frac{1}{|M|^{N' n_t}} \int_{\mathbf{x}} \frac{\partial^2}{\partial f_D^2} \left( \ln \sum_{i=1}^{|M|^{N' n_t}} \frac{\exp\left(-\frac{1}{2} \mathbf{x}^\dagger \boldsymbol{\Sigma}^{-1}(\mathbf{c}_{(i)}, \boldsymbol{\varphi}) \mathbf{x}\right)}{\det^{\frac{1}{2}}(\boldsymbol{\Sigma}(\mathbf{c}_{(i)}, \boldsymbol{\varphi}))}\right) \sum_{q=1}^{|M|^{N' n_t}} \frac{\exp\left(-\frac{1}{2} \mathbf{x}^\dagger \boldsymbol{\Sigma}^{-1}(\mathbf{c}_{(q)}, \boldsymbol{\varphi}) \mathbf{x}\right)}{(2\pi)^{N n_r} \det^{\frac{1}{2}}(\boldsymbol{\Sigma}(\mathbf{c}_{(q)}, \boldsymbol{\varphi}))} d\mathbf{x}. \quad (19)$$

## B. NDA-CRLB

Let us consider that the symbols transmitted by each antenna are selected from a constellation with elements  $\{c_1 \ c_2 \ \dots \ c_{|M|}\}$ , where  $\frac{1}{|M|} \sum_{i=1}^{|M|} |c_i|^2 = 1$ . The PDF of the received vector  $\mathbf{r}$  for NDA-MDS estimation is expressed as

$$p(\mathbf{r}; \boldsymbol{\varphi}) = \sum_{\mathbf{c}} p(\mathbf{r}, \mathbf{c}; \boldsymbol{\varphi}), \quad (13)$$

where  $\mathbf{c}$  is the constellation vector as  $\mathbf{c} \triangleq [\mathbf{c}^{(1)\dagger} \ \mathbf{c}^{(2)\dagger} \ \dots \ \mathbf{c}^{(n_t)\dagger}]^\dagger$ ,  $\mathbf{c}^{(m)} \triangleq [\bar{c}_{1-L}^{(m)} \ \bar{c}_{2-L}^{(m)} \ \dots \ \bar{c}_{N-1}^{(m)} \ \check{c}_{1-L}^{(m)} \ \check{c}_{2-L}^{(m)} \ \dots \ \check{c}_{N-1}^{(m)}]^\dagger$ ,  $c_k^{(m)} = \bar{c}_k^{(m)} + j\check{c}_k^{(m)}$  is the constellation point of the  $m$ th transmit antenna at time  $k$ , and  $\boldsymbol{\varphi} \triangleq [\boldsymbol{\beta}^\dagger \ \boldsymbol{\xi}^\dagger \ \boldsymbol{\vartheta}^\dagger \ f_D]^\dagger$  with  $\boldsymbol{\beta} \triangleq [\sigma_{s_1}^2 \ \sigma_{s_2}^2 \ \dots \ \sigma_{s_{n_t}}^2]^\dagger$ , and  $\boldsymbol{\xi}$  and  $\boldsymbol{\vartheta}$  are given in (7).

By employing the chain rule of probability and using  $p(\mathbf{c} = \mathbf{c}_{\langle i \rangle}) = |M|^{-N' n_t}$ ,  $N' \triangleq N + L - 1$ , one can write (13) as

$$\begin{aligned} p(\mathbf{r}; \boldsymbol{\varphi}) &= \sum_{\mathbf{c}} p(\mathbf{r}, \mathbf{c}; \boldsymbol{\varphi}) = \sum_{\mathbf{c}} p(\mathbf{c} = \mathbf{c}) p(\mathbf{r} | \mathbf{c} = \mathbf{c}; \boldsymbol{\varphi}) \\ &= \frac{1}{|M|^{N' n_t}} \sum_{i=1}^{|M|^{N' n_t}} p(\mathbf{r} | \mathbf{c} = \mathbf{c}_{\langle i \rangle}; \boldsymbol{\varphi}), \end{aligned} \quad (14)$$

where  $\mathbf{c}_{\langle i \rangle}$  represents the  $i$ th possible constellation vector at the transmit-side.

Similar to the DA-CRLB,  $p(\mathbf{r} | \mathbf{c} = \mathbf{c}_{\langle i \rangle}; \boldsymbol{\varphi})$  is Gaussian and

$$p(\mathbf{r} | \mathbf{c} = \mathbf{c}_{\langle i \rangle}; \boldsymbol{\varphi}) = \frac{\exp\left(-\frac{1}{2} \mathbf{r}^\dagger \boldsymbol{\Sigma}^{-1}(\mathbf{c}_{\langle i \rangle}, \boldsymbol{\varphi}) \mathbf{r}\right)}{(2\pi)^{N n_r} \det^{\frac{1}{2}}(\boldsymbol{\Sigma}(\mathbf{c}_{\langle i \rangle}, \boldsymbol{\varphi}))}, \quad (15)$$

where  $\boldsymbol{\Sigma}(\mathbf{c}_{\langle i \rangle}, \boldsymbol{\varphi}) \triangleq \mathbb{E}\{\mathbf{r}_{\langle i \rangle} \mathbf{r}_{\langle i \rangle}^\dagger\}$  is the covariance matrix of the received vector  $\mathbf{r}_{\langle i \rangle}$  given the constellation vector is  $\mathbf{c} = \mathbf{c}_{\langle i \rangle}$ ,  $i = 1, 2, \dots, |M|^{N' n_t}$ . The  $2N n_r \times 2N n_r$  covariance matrix  $\boldsymbol{\Sigma}(\mathbf{c}_{\langle i \rangle}, \boldsymbol{\varphi})$  is block diagonal as in (8), where its diagonal elements, i.e.,  $\boldsymbol{\Sigma}_{\langle i \rangle}^{(n)} \triangleq \mathbb{E}\{\mathbf{r}_{\langle i \rangle}^{(n)} \mathbf{r}_{\langle i \rangle}^{(n)\dagger}\}$ ,  $n \in \{1, 2, \dots, n_r\}$ , are obtained as

$$\begin{aligned} \mathbb{E}\{\bar{r}_{k, \langle i \rangle}^{(n)} \bar{r}_{k+u, \langle i \rangle}^{(n)}\} &= \mathbb{E}\{\check{r}_{k, \langle i \rangle}^{(n)} \check{r}_{k, \langle i \rangle}^{(n)}\} \\ &= \frac{1}{2} \sum_{m=1}^{n_t} \sum_{l=1}^L \sigma_{h(mn), l}^2 \sigma_{s_m}^2 \left( \bar{c}_{k-l, \langle i \rangle}^{(m)} \bar{c}_{k+u-l, \langle i \rangle}^{(m)} \right. \\ &\quad \left. + \check{c}_{k-l, \langle i \rangle}^{(m)} \check{c}_{k+u-l, \langle i \rangle}^{(m)} \right) J_0(2\pi f_D T_s u) + \frac{\sigma_{w_n}^2}{2} \delta_{u,0} \end{aligned} \quad (16a)$$

$$\begin{aligned} \mathbb{E}\{\bar{r}_{k, \langle i \rangle}^{(n)} \check{r}_{k+u, \langle i \rangle}^{(n)}\} &= -\mathbb{E}\{\check{r}_{k, \langle i \rangle}^{(n)} \bar{r}_{k, \langle i \rangle}^{(n)}\} \\ &= \frac{1}{2} \sum_{m=1}^{n_t} \sum_{l=1}^L \sigma_{h(mn), l}^2 \sigma_{s_m}^2 \left( \bar{c}_{k-l, \langle i \rangle}^{(m)} \check{c}_{k+u-l, \langle i \rangle}^{(m)} \right. \\ &\quad \left. - \check{c}_{k-l, \langle i \rangle}^{(m)} \bar{c}_{k+u-l, \langle i \rangle}^{(m)} \right) J_0(2\pi f_D T_s u). \end{aligned} \quad (16b)$$

By substituting (15) into (14), one obtains

$$p(\mathbf{r}; \boldsymbol{\varphi}) = \frac{1}{|M|^{N' n_t}} \sum_{i=1}^{|M|^{N' n_t}} \frac{\exp\left(-\frac{1}{2} \mathbf{r}^\dagger \boldsymbol{\Sigma}^{-1}(\mathbf{c}_{\langle i \rangle}, \boldsymbol{\varphi}) \mathbf{r}\right)}{(2\pi)^{N n_r} \det^{\frac{1}{2}}(\boldsymbol{\Sigma}(\mathbf{c}_{\langle i \rangle}, \boldsymbol{\varphi}))}. \quad (17)$$

Finally, by employing (17), the NDA-CRLB for MDS estimation in MIMO frequency-selective fading channel is expressed as

$$\text{Var}(\hat{f}_D) \geq I^{-1}(f_D) = \frac{1}{-\mathbb{E}\left\{\frac{\partial^2 \ln p(\mathbf{r}; \boldsymbol{\varphi})}{\partial f_D^2}\right\}}, \quad (18)$$

where  $I(f_D)$  is given in (19) on the top of this page, and  $\int_{\mathbf{x}} \triangleq \int_{x_1} \int_{x_2} \dots \int_{x_{2N n_r}}$ . As seen, there is no an explicit expression for (19), and thus, for the CRLB in (18). Therefore, numerical methods are used to solve (19) and (18).

$$\begin{aligned}
\kappa_u^{(n)} &= \mathbb{E} \left\{ |r_k^{(n)}|^2 |r_{k+u}^{(n)}|^2 \right\} = \sum_{m=1}^{n_t} \sum_{l=1}^L \mathbb{E} \left\{ |h_{k,l}^{(mn)}|^2 |h_{k+u,l}^{(mn)}|^2 \right\} \sigma_{s_m}^4 + \sum_{m_1=1}^{n_t} \sum_{m_2 \neq m_1}^{n_t} \sum_{l=1}^L \mathbb{E} \left\{ |h_{k,l}^{(m_1 n)}|^2 |h_{k+u,l}^{(m_2 n)}|^2 \right\} \sigma_{s_{m_1}}^2 \sigma_{s_{m_2}}^2 \\
&+ \sum_{m=1}^{n_t} \sum_{l_1=1}^L \sum_{l_2 \neq l_1}^L \mathbb{E} \left\{ |h_{k,l_1}^{(mn)}|^2 |h_{k+u,l_2}^{(mn)}|^2 \right\} \sigma_{s_m}^4 + \sum_{m_1=1}^{n_t} \sum_{m_2 \neq m_1}^{n_t} \sum_{l_1=1}^L \sum_{l_2 \neq l_1}^L \mathbb{E} \left\{ |h_{k,l_1}^{(m_1 n)}|^2 |h_{k+u,l_2}^{(m_2 n)}|^2 \right\} \sigma_{s_{m_1}}^2 \sigma_{s_{m_2}}^2 \\
&+ 2\sigma_{w_n}^2 \sum_{m=1}^{n_t} \sum_{l=1}^L \mathbb{E} \left\{ |h_{k,l}^{(mn)}|^2 \right\} \sigma_{s_m}^2 + \sigma_{w_n}^4, \quad u \geq L.
\end{aligned} \tag{28}$$


---

#### IV. ML ESTIMATION FOR MDS

In this section, we derive the DA- and NDA-MLEs for MDS in MIMO frequency-selective fading channel.

##### A. DA-MLE for MDS

The DA-MLE for  $f_D$  is obtained as

$$\hat{f}_D = \arg \max_{f_D} p(\mathbf{r}|\mathbf{s}; \boldsymbol{\theta}), \tag{20}$$

where  $p(\mathbf{r}|\mathbf{s}; \boldsymbol{\theta})$  is given in (6). Since  $p(\mathbf{r}|\mathbf{s}; \boldsymbol{\theta})$  is a differentiable function, the DA-MLE for  $f_D$  is obtained from

$$\frac{\partial \ln p(\mathbf{r}|\mathbf{s}; \boldsymbol{\theta})}{\partial f_D} = 0. \tag{21}$$

By substituting (6) into (21) and after some mathematical manipulations, one obtains

$$\begin{aligned}
\frac{\partial \ln p(\mathbf{r}|\mathbf{s}; \boldsymbol{\theta})}{\partial f_D} &= -\frac{1}{2} \text{tr} \left[ \boldsymbol{\Sigma}^{-1}(\mathbf{s}, \boldsymbol{\theta}) \frac{\partial \boldsymbol{\Sigma}(\mathbf{s}, \boldsymbol{\theta})}{\partial f_D} \right] \\
&+ \frac{1}{2} \mathbf{r}^\dagger \boldsymbol{\Sigma}^{-1}(\mathbf{s}, \boldsymbol{\theta}) \frac{\partial \boldsymbol{\Sigma}(\mathbf{s}, \boldsymbol{\theta})}{\partial f_D} \boldsymbol{\Sigma}^{-1}(\mathbf{s}, \boldsymbol{\theta}) \mathbf{r}.
\end{aligned} \tag{22}$$

As seen in (22), there is no closed-form solution for (21). Thus, numerical methods need to be used to obtain solution. By employing the Fisher-scoring method [42],<sup>2</sup> the solution of (22) can be iteratively obtained as

$$\hat{f}_D^{[t+1]} = \hat{f}_D^{[t]} + I^{-1}(f_D) \frac{\partial \ln p(\mathbf{r}|\mathbf{s}; \boldsymbol{\theta})}{\partial f_D} \Big|_{f_D = \hat{f}_D^{[t]}}, \tag{23}$$

where  $I(f_D)$  and  $\frac{\partial \ln p(\mathbf{r}|\mathbf{s}; \boldsymbol{\theta})}{\partial f_D}$  are given in (11) and (22), respectively.

##### B. NDA-MLE for MDS

Similar to the DA-MLE, the NDA-MLE for MDS is obtained from

$$\hat{f}_D = \arg \max_{f_D} p(\mathbf{r}; \boldsymbol{\varphi}), \tag{24}$$

<sup>2</sup>The Fisher-scoring method replaces the Hessian matrix in the Newtown-Raphson method with the negative of the Fisher information matrix [43].

where  $p(\mathbf{r}; \boldsymbol{\varphi})$  is given in (17). Since  $p(\mathbf{r}; \boldsymbol{\varphi})$  is a linear combination of differentiable functions, the NDA-MLE for  $f_D$  is obtained from

$$\frac{\partial \ln p(\mathbf{r}; \boldsymbol{\varphi})}{\partial f_D} = 0. \quad (25)$$

By substituting (17) into (25) and after some algebra, one obtains

$$\sum_{i=1}^{|\mathcal{M}|^{N'_{nt}}} \left\{ \frac{\mathbf{r}^\dagger \boldsymbol{\Sigma}^{-1}(\mathbf{c}_{\langle i \rangle}, \boldsymbol{\varphi}) \frac{\partial \boldsymbol{\Sigma}(\mathbf{c}_{\langle i \rangle}, \boldsymbol{\varphi})}{\partial f_D} \boldsymbol{\Sigma}^{-1}(\mathbf{c}_{\langle i \rangle}, \boldsymbol{\varphi}) \mathbf{r}}{\det^{\frac{1}{2}} \boldsymbol{\Sigma}(\mathbf{c}_{\langle i \rangle}, \boldsymbol{\varphi})} - \frac{\text{tr} \left[ \boldsymbol{\Sigma}^{-1}(\mathbf{c}_{\langle i \rangle}, \boldsymbol{\varphi}) \frac{\partial \boldsymbol{\Sigma}(\mathbf{c}_{\langle i \rangle}, \boldsymbol{\varphi})}{\partial f_D} \right]}{\det^{\frac{1}{2}} \boldsymbol{\Sigma}(\mathbf{c}_{\langle i \rangle}, \boldsymbol{\varphi})} \right\} = 0 \quad (26)$$

Similar to the DA-MLE, there is no closed-form solution for (26); thus, numerical methods are used to solve (26).

## V. NDA-MOMENT-BASED (MB) ESTIMATION OF MDS

In this section, we propose an NDA-MB MDS estimator for multiple input single output (MISO) systems under frequency-selective Rayleigh fading channel by employing the fourth-order moment of the received signal. Then, an extension of the proposed estimator to the MIMO systems is provided.

### A. NDA-MBE for MDS in MISO Systems

Let us assume that the parameter vector  $\boldsymbol{\varphi} = [\boldsymbol{\beta}^\dagger \ \boldsymbol{\xi}^\dagger \ \boldsymbol{\vartheta}^\dagger \ f_D]^\dagger$  is unknown at the receive-side. The statistical MB approach enables us to propose an NDA-MBE to estimate  $f_D$  without any priori knowledge of  $\boldsymbol{\beta}$ ,  $\boldsymbol{\xi}$ , and  $\boldsymbol{\vartheta}$ . Let us consider the fourth-order two-conjugate moment of the received signal at the  $n$ th receive antenna, defined as

$$\kappa_u^{(n)} \triangleq \mathbb{E} \left\{ |r_k^{(n)}|^2 |r_{k+u}^{(n)}|^2 \right\}. \quad (27)$$

With the transmitted symbols,  $s_k^{(m)}$ ,  $m = 1, \dots, n_t$  being independent, drawn from symmetric complex-valued constellation points,<sup>3</sup> and with  $u \geq L$ ,  $\kappa_u^{(n)}$  is expressed as in (28) at the top of this page (see Appendix I for proof).

By employing the first-order autoregressive model of the Rayleigh fading channel, one can write [45], [46]

$$h_{k,l}^{(mn)} = \Psi_u h_{k+u,l}^{(mn)} + v_{k,l}^{(mn)}, \quad (29)$$

where  $\Psi_u \triangleq J_0(2\pi f_D T_s u)$  and  $v_{k,l}^{(mn)}$  is a zero-mean complex-valued Gaussian white process with variance  $\mathbb{E}\{|v_{k,l}^{(mn)}|^2\} = (1 - |\Psi_u|^2) \sigma_{h_{(mn),l}^{(mn)}}^2$ , which is independent of  $h_{k,l}^{(mn)}$ .

By using (29) and exploiting the property of a complex-valued Gaussian random variable  $z \sim \mathcal{N}_c(0, \sigma_z^2)$  that  $\mathbb{E}\{|z|^{2n}\} = n! \sigma_z^{2n}$  [47], one obtains

$$\begin{aligned} & \mathbb{E} \left\{ |h_{k,l}^{(mn)}|^2 |h_{k+u,l}^{(mn)}|^2 \right\} \\ &= \mathbb{E} \left\{ \left| (J_0(2\pi f_D T_s u) h_{k+u,l}^{(mn)} + v_{k,l}^{(mn)}) \right|^2 |h_{k+u,l}^{(mn)}|^2 \right\} \end{aligned} \quad (30)$$

<sup>3</sup> $\mathbb{E}\{(s_k^{(m)})^2\} = 0$  for  $M$ -ary phase-shift-keying (PSK) and quadrature amplitude modulation (QAM),  $M > 2$  [44].

$$\begin{aligned}
&= J_0^2(2\pi f_d T_s u) \mathbb{E} \left\{ |h_{k+u,l}^{(mn)}|^4 \right\} + \mathbb{E} \left\{ |v_{k,l}^{(mn)}|^2 |h_{k+u,l}^{(mn)}|^2 \right\} \\
&\quad + J_0(2\pi f_d T_s u) \mathbb{E} \left\{ |h_{k+u,l}^{(mn)}|^2 |h_{k+u,l}^{(mn)}|^2 (v_{k,l}^{(mn)})^* \right\} \\
&\quad + J_0(2\pi f_d T_s u) \mathbb{E} \left\{ (h_{k+u,l}^{(mn)})^* |h_{k+u,l}^{(mn)}|^2 (v_{k,l}^{(mn)}) \right\} \\
&= 2J_0^2(2\pi f_d T_s u) \sigma_{h_{(mn),l}}^4 + (1 - J_0^2(2\pi f_d T_s u)) \sigma_{h_{(mn),l}}^4 \\
&= (1 + J_0^2(2\pi f_d T_s u)) \sigma_{h_{(mn),l}}^4 \quad m = 1, \dots, n_t, \quad l = 1, \dots, L.
\end{aligned}$$

With the channel taps  $l_1$  and  $l_2$  being uncorrelated for each transmit antenna, i.e.,  $\mathbb{E} \{ h_{k,l_1}^{(mn)} (h_{k,l_2}^{(mn)})^* \} = \sigma_{h_{(mn),l_1}}^2 \delta_{l_1,l_2}$  and employing

$$\begin{aligned}
&\mathbb{E} \left\{ |h_{k,l_1}^{(m_1 n)}|^2 |h_{k+u,l_2}^{(m_2 n)}|^2 \right\} \tag{31} \\
&= \sigma_{h_{(m_1 n),l_1}}^2 \sigma_{h_{(m_2 n),l_2}}^2 \left[ (1 - \delta_{l_1,l_2})(1 - \delta_{m_1,m_2}) \right. \\
&\quad \left. + \delta_{l_1,l_2}(1 - \delta_{m_1,m_2}) + (1 - \delta_{l_1,l_2})\delta_{m_1,m_2} \right] \\
&\quad + \sigma_{h_{(m_1 n),l_1}}^4 (1 + J_0^2(2\pi f_d T_s u)) \delta_{m_1,m_2} \delta_{l_1,l_2},
\end{aligned}$$

one can write (28) as

$$\begin{aligned}
\kappa_u^{(n)} &= \sum_{m=1}^{n_t} \sum_{l=1}^L \sigma_{h_{(mn),l}}^4 \sigma_{s_m}^4 (1 + J_0^2(2\pi f_d T_s u)) \tag{32} \\
&\quad + \sum_{m_1=1}^{n_t} \sum_{m_2 \neq m_1}^{n_t} \sum_{l=1}^L \sigma_{h_{(m_1 n),l}}^2 \sigma_{h_{(m_2 n),l}}^2 \sigma_{s_{m_1}}^2 \sigma_{s_{m_2}}^2 \\
&\quad + \sum_{m=1}^{n_t} \sum_{l_1=1}^L \sum_{l_2 \neq l_1}^L \sigma_{h_{(mn),l_1}}^2 \sigma_{h_{(mn),l_2}}^2 \sigma_{s_m}^4 \\
&\quad + \sum_{m_1=1}^{n_t} \sum_{m_2 \neq m_1}^{n_t} \sum_{l_1=1}^L \sum_{l_2 \neq l_1}^L \sigma_{h_{(m_1 n),l_1}}^2 \sigma_{h_{(m_2 n),l_2}}^2 \sigma_{s_{m_1}}^2 \sigma_{s_{m_2}}^2 \\
&\quad + 2\sigma_{w_n}^2 \sum_{m=1}^{n_t} \sum_{l=1}^L \sigma_{h_{(mn),l}}^2 \sigma_{s_m}^2 + \sigma_{w_n}^4.
\end{aligned}$$

$$\hat{f}_D^{[t+1]} = \hat{f}_D^{[t]} - \frac{\sum_{u=U_{\min}}^{M_{\max}} 8\pi T_s u \left( \hat{\Psi}_u^{(n)} - J_0^2(2\pi f_D^{[t]} T_s u) \right) J_0(2\pi f_D^{[t]} T_s u) J_1(2\pi f_D^{[t]} T_s u)}{\frac{\partial^2}{\partial f_D^2} \sum_{u=U_{\min}}^{U_{\max}} \left( \hat{\Psi}_u^{(n)} - J_0^2(2\pi f_D T_s u) \right)^2 \Big|_{f_D=f_D^{[t]}}} \tag{42}$$

$$\begin{aligned}
\frac{\partial^2}{\partial f_D^2} \sum_{u=U_{\min}}^{U_{\max}} \left( \hat{\Psi}_u - J_0^2(2\pi f_D T_s u) \right)^2 \Big|_{f_D=f_D^{[t]}} &= \sum_{u=U_{\min}}^{M_{\max}} \left\{ 32\pi^2 T_s^2 u^2 J_0^2(2\pi f_D^{[t]} T_s u) J_1^2(2\pi f_D^{[t]} T_s u) \right. \\
&\quad \left. + 8\pi T_s u \left( 2\pi T_s u \left( J_0^2(2\pi f_D^{[t]} T_s u) - J_1^2(2\pi f_D^{[t]} T_s u) \right) - \frac{J_0(2\pi f_D^{[t]} T_s u) J_1(2\pi f_D^{[t]} T_s u)}{f_D^{[t]}} \right) \left( \hat{\Psi}_u^{(n)} - J_0^2(2\pi f_D^{[t]} T_s u) \right) \right\}
\end{aligned}$$


---

Further, let us consider the second-order moment of the received signal, i.e.,  $\mu_2^{(n)} \triangleq \mathbb{E}\{|r_k^{(n)}|^2\}$ . By using (1), it can be easily shown that

$$\mu_2^{(n)} = \sum_{m=1}^{n_t} \sum_{l=1}^L \sigma_{h_{(mn),l}}^2 \sigma_{s_m}^2 + \sigma_{w_n}^2. \quad (33)$$

By employing (32) and (33), one obtains the normalized squared AF of the fading channel as (see Appendix II for proof)

$$\Psi_u \triangleq J_0^2(2\pi f_d T_s u) = \eta^{(n)} \left( \kappa_u^{(n)} - \left( \mu_2^{(n)} \right)^2 \right), \quad (34)$$

where  $\eta^{(n)} = 1 / \sum_{m=1}^{n_t} \sum_{l=1}^L \sigma_{h_{(mn),l}}^4 \sigma_{s_m}^4$ .

For non-constant modulus constellations,  $\eta^{(n)}$  is expressed in terms of  $\mu_4^{(n)} \triangleq \mathbb{E}\{|r_k^{(n)}|^4\}$  and  $\mu_2^{(n)}$  as (see Appendix III for proof)

$$\eta^{(n)} = \frac{2(\Omega_s - 1)}{\mu_4^{(n)} - 2\left(\mu_2^{(n)}\right)^2}, \quad (35)$$

where  $\Omega_s = \frac{1}{|M|} \sum_{i=1}^{|M|} |c_i|^4$  is a constant, and  $1 < \Omega_s \leq 2$ .<sup>4</sup>

Finally, substituting (35) into (34) yields

$$\Psi_u \triangleq 2(\Omega_s - 1) \frac{\kappa_u^{(n)} - \left(\mu_2^{(n)}\right)^2}{\mu_4^{(n)} - 2\left(\mu_2^{(n)}\right)^2}. \quad (36)$$

As seen, the normalized squared AF of the fading channel is expressed as a non-linear function of the  $\mu_2^{(n)}$ ,  $\mu_4^{(n)}$ , and  $\kappa_u^{(n)}$ . In practice, statistical moments are estimated by time averages of the received signal. For (36), the following estimators of the moments are employed

$$\begin{aligned} \hat{\mu}_2^{(n)} &= \frac{1}{N} \sum_{k=1}^N |r_k^{(n)}|^2 \\ \hat{\mu}_4^{(n)} &= \frac{1}{N} \sum_{k=1}^N |r_k^{(n)}|^4 \\ \hat{\kappa}_u^{(n)} &= \frac{1}{N-u} \sum_{k=1}^{N-u} |r_k^{(n)}|^2 |r_{k+u}^{(n)}|^2, \end{aligned} \quad (37)$$

where  $u \geq L > 0$ .

By substituting the corresponding estimators in (36), the estimate of the normalized squared AF is given as

$$\hat{\Psi}_u^{(n)} \triangleq 2(\Omega_s - 1) \frac{\hat{\kappa}_u^{(n)} - \left(\hat{\mu}_2^{(n)}\right)^2}{\hat{\mu}_4^{(n)} - 2\left(\hat{\mu}_2^{(n)}\right)^2}. \quad (38)$$

Now, based on (34) and (38), the problem of MDS estimation can be formulated as a non-linear regression problem. Given the estimated normalized squared AF,  $\hat{\Psi}_u^{(n)}$ , the non-linear regression model assumes that the relationship between  $\hat{\Psi}_u^{(n)}$  and

<sup>4</sup>For 16-QAM, 64-QAM, and complex-valued zero-mean Gaussian signals,  $\Omega_s$  is 1.32, 1.38, and 2, respectively [44].

$\Psi_u$  is modeled through a disturbance term or error variable  $\epsilon_u^{(n)}$  as [48], [49]

$$\begin{aligned}\hat{\Psi}_u^{(n)} &= \Psi_u + \epsilon_u^{(n)} \\ &= J_0^2(2\pi f_D T_s u) + \epsilon_u^{(n)}, \quad u = U_{\min}, \dots, U_{\max},\end{aligned}\tag{39}$$

where  $U_{\min}$  and  $U_{\max}$  are the maximum and minimum delay lags, respectively.

To solve the non-linear regression problem in (39), the LS curve-fitting optimization technique is employed. Based on the LS curve-fitting optimization, the estimate of  $f_D$ , i.e.,  $\hat{f}_D$ , is obtained through minimizing the sum of the squared residuals (SSR) as [49]

$$\begin{aligned}\underset{f_D}{\text{minimize}} \quad & \sum_{u=U_{\min}}^{U_{\max}} \left( \hat{\Psi}_u^{(n)} - J_0^2(2\pi f_D T_s u) \right)^2 \\ \text{subject to} \quad & f_l \leq f_D \leq f_h,\end{aligned}\tag{40}$$

where  $f_l$  and  $f_h$  are the minimum and maximum possible MDSs, respectively. To obtain  $\hat{f}_D$ , we consider the derivative of the SSR with respect to  $f_D$  and set it equal to zero as follows:

$$\begin{aligned}\sum_{u=U_{\min}}^{M_{\max}} 8\pi T_s u \left( \hat{\Psi}_u^{(n)} - J_0^2(2\pi f_D T_s u) \right) \\ J_0(2\pi f_D T_s u) J_1(2\pi f_D T_s u) = 0.\end{aligned}\tag{41}$$

As seen, for the non-linear regression, the derivative in (41) is a function of  $f_D$ . Thus, an explicit solution for  $\hat{f}_D$  cannot be obtained. However, numerical methods [50] can be employed to solve the LS curve-fitting optimization problem in (40).

By employing the Newton-Raphson method,  $\hat{f}_D$  can be iteratively obtained as it is shown in (42) at the top of next page. The main problem with the Newton-Raphson method is that it suffers from the convergence problem [43]. Since the parameter space for the MDS estimation is one-dimensional, the grid search method can be employed, which ensures the global optimality of the solution. With the grid search method, the parameter space, i.e.,  $[f_l, f_h]$  is discretized as a grid with step size  $\delta$ , and the value which minimizes SSR is considered as the estimated  $f_D$ . This procedure can be performed in two steps, including a rough estimate of the MDS,  $\hat{f}_D^{(r)}$ , by choosing a larger step size  $\Delta$  followed by a fine estimate,  $\hat{f}_D^{(s)}$ , through small grid step size  $\delta$  around the rough estimate, i.e.,  $[\hat{f}_D^{(r)} - \Delta, \hat{f}_D^{(r)} + \Delta]$ . A formal description of the proposed NDA-MBE for MDS in MISO frequency-selective channel is presented in Algorithm 1.

It is worth noting that  $f_D$  can be estimated by using a downsampled version of  $\hat{\Psi}_u^{(n)}$ . For the case of uniform downsampling, i.e.,  $u = \ell u_s$ , the SSR is given as

$$\sum_{\ell=0}^{N_{1a}-1} \left( \hat{\Psi}_{U_{\min} + \ell u_s}^{(n)} - \Psi_{U_{\min} + \ell u_s} \right)^2,\tag{43}$$

where  $u_s$  is the downsampling period expressed in delay lags,  $N_{1a}$  is the number of delay lags,

$$\Psi_{\ell u_s} = J_0^2 \left( 2\pi f_D T_s (U_{\min} + \ell u_s) \right),\tag{44}$$

---

**Algorithm 1** : NDA-MBE for MDS in MISO systems
 

---

- 1: Set  $f_l$ ,  $f_h$ ,  $\Delta$ , and  $\delta$
  - 2: Acquire the measurements  $\{r_k^{(n)}\}_{k=1}^N$
  - 3: Estimate the statistics  $\hat{\mu}_2^{(n)}$ ,  $\hat{\mu}_4^{(n)}$ , and  $\hat{\kappa}_u^{(n)}$ , by employing (37)
  - 4: Compute  $\hat{\Psi}_u^{(n)}$ ,  $\forall u \in \{U_{\min}, \dots, U_{\max}\}$  by using (38)
  - 5: Obtain  $\hat{f}_D^{(r)}$  by solving the minimization problem in (40) through the grid search method with grid step size  $\Delta$
  - 6: Obtain  $\hat{f}_D^{(s)}$  by solving the minimization problem in (40) through the grid search method over  $[\hat{f}_D^{(r)} - \Delta, \hat{f}_D^{(r)} + \Delta]$  with grid step size  $\delta$
  - 7:  $\hat{f}_D = \hat{f}_D^{(s)}$
- 

and

$$\hat{\Psi}_{U_{\min} + \ell u_s}^{(n)} = 2(\Omega_s - 1) \frac{\hat{\kappa}_{U_{\min} + \ell u_s}^{(n)} - (\hat{\mu}_2^{(n)})^2}{\hat{\mu}_4^{(n)} - 2(\hat{\mu}_2^{(n)})^2}. \quad (45)$$

The downsampled version of  $\hat{\Psi}_u^{(n)}$  is usually employed for the rough MDS estimation, where  $\Delta$  is a large value.

### B. NDA-MBE for MDS in MIMO Systems

The performance of the proposed NDA-MBE for MDS in MISO system can be improved when employing multiple receive antennas due to the spatial diversity, by combining the estimated normalized squared AFs,  $\hat{\Psi}_u^{(n)}$ ,  $n = 1, \dots, n_r$  as

$$\tilde{\Psi}_u = \sum_{n=1}^{n_r} \lambda_u^{(n)} \hat{\Psi}_u^{(n)}, \quad (46)$$

where  $\Lambda_u \triangleq [\lambda_u^{(1)} \lambda_u^{(2)} \dots \lambda_u^{(n_r)}]^\dagger$ , with  $\sum_{n=1}^{n_r} \lambda_u^{(n)} = 1$ , is the weighting vector. Let us define  $\hat{\Psi}_u \triangleq [\hat{\Psi}_u^{(1)} \hat{\Psi}_u^{(2)} \dots \hat{\Psi}_u^{(n_r)}]^\dagger$ .

The mean square error (MSE) of the combined normalized squared AF in (46) is expressed as

$$\mathbb{E}\{(\tilde{\Psi}_u - \Psi_u)^2\} = \Lambda_u^\dagger C_u \Lambda_u + (\Lambda_u^\dagger \mu_u - \Psi_u)^2, \quad (47)$$

where  $C_u \triangleq \mathbb{E}\{(\hat{\Psi}_u - \mu_u)(\hat{\Psi}_u - \mu_u)^\dagger\}$  and  $\mu_u \triangleq \mathbb{E}\{\hat{\Psi}_u\}$ .

By employing the method of Lagrange multipliers, the optimal weighting vector  $\Lambda_u^{\text{op}}$  in (47) in terms of minimum MSE is obtained as

$$\Lambda_u^{\text{op}} = (\mathbf{1}^\dagger \mathbf{y}_u)^{-1} \mathbf{y}_u, \quad (48)$$

where  $\mathbf{y}_u \triangleq (C_u + (\mu_u - \Psi_u \mathbf{1})(\mu_u - \Psi_u \mathbf{1})^\dagger)^{-1} \mathbf{1}$  and  $\mathbf{1} \triangleq [1 \ 1 \ \dots \ 1]^\dagger$  is an  $n_r$ -dimensional vector of ones.

As seen, the optimal weighting vector,  $\Lambda_u^{\text{op}}$ , in (48) depends on the true value of MDS, i.e.,  $f_D$ , through the true normalized squared AF,  $\Psi_u$ , in  $\mathbf{y}_u$ . To obtain the optimal weighting vector, the mean vector  $\mu_u$  and covariance matrix  $C_u$  are required to be estimated from the received symbols. One approach is bootstrapping [51]–[53]. The bootstrap method suggests to re-sample the empirical joint cumulative distribution function (CDF) of  $\hat{\Psi}_u$  to estimate  $\mu_u$  and  $C_u$  as summarized in Algorithm 2.<sup>5</sup>

<sup>5</sup>Since  $\hat{\Psi}_u^{(n)}$ ,  $n = 1, \dots, n_r$  are uncorrelated random variables,  $C_u$  is a diagonal matrix. Thus, only the diagonal elements of  $\hat{C}_u$  are employed to obtain the optimal weighting vector.

---

**Algorithm 2** : Bootstrap Algorithm for Optimal Combining
 

---

- 1: Set  $N_B$
- 2: **for**  $t = 1, 2, \dots, N_B$  **do**
- 3:   Draw a random sample of size  $N$ , with replacement, from  $\mathcal{X} \triangleq \{1, 2, \dots, N\}$  and name it  $\mathcal{X}^*$
- 4:   **for**  $n = 1, 2, \dots, n_r$  **do**

$$\hat{\Psi}_u^{(n)*}[t] = \frac{\frac{1}{N-u} \sum_{k \in \mathcal{X}^*} |r_k^{(n)}|^2 |r_{k+u}^{(n)}|^2 - \left( \frac{1}{N} \sum_{k \in \mathcal{X}^*} |r_k^{(n)}|^2 \right)^2}{\frac{1}{N} \sum_{k \in \mathcal{X}^*} |r_k^{(n)}|^4 - 2 \left( \frac{1}{N} \sum_{k \in \mathcal{X}^*} |r_k^{(n)}|^2 \right)^2}$$

- 5:   **end for**
  - 6:    $\hat{\Psi}_u^*[t] \triangleq 2(\Omega_s - 1) [\hat{\Psi}_u^{(1)*} \hat{\Psi}_u^{(2)*} \dots \hat{\Psi}_u^{(n_r)*}]^\dagger$
  - 7: **end for**
  - 8:  $\Gamma_u = [\hat{\Psi}_u^*[1] \hat{\Psi}_u^*[2] \dots \hat{\Psi}_u^*[N_B]]$
  - 9:  $\hat{\mu}_u = \frac{1}{N_B} \sum_{t=1}^{N_B} \hat{\Psi}_u^*[t]$
  - 10:  $\hat{C}_u = \frac{1}{N_B - 1} (\Gamma_u - \hat{\mu}_u \mathbf{1}^\dagger) (\Gamma_u - \hat{\mu}_u \mathbf{1}^\dagger)^\dagger$
- 

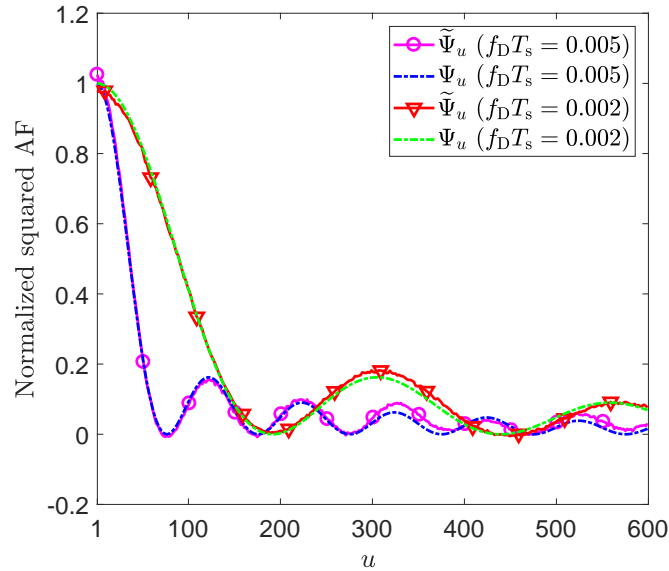


Fig. 1. Illustration of the non-linear LS regression for the uniformly sampled normalized squared AF for  $f_D T_s = 0.02$  and  $f_D T_s = 0.005$ , with  $n_t = 1$ ,  $n_r = 2$ ,  $L = 1$ ,  $u_s = 2$ , and at  $\gamma = 10$  dB.

As seen in Algorithm 2, the optimal weighting vector for each delay lag  $u$  is derived at the expense of higher computational complexity. In order to avoid this computational complexity, the suboptimal equal weight combining method can be employed as

$$\tilde{\Psi}_u = \frac{1}{n_r} \sum_{n=1}^{n_r} \hat{\Psi}_u^{(n)}. \quad (49)$$

Fig. 1 shows how  $\tilde{\Psi}_u$  fits  $\Psi_u$  through the equal weight combining in (49) for  $f_d T_s = 0.02$  and  $f_d T_s = 0.005$  with  $n_t = 1$ ,  $n_r = 2$ ,  $L = 1$ ,  $u_s = 2$ , and at  $\gamma = 10$  dB.

Finally, similar to the MISO scenario, the problem of MDS estimation for multiple receive antennas is formulated as non-linear regression problem in (39) for  $\tilde{\Psi}_u$ . A formal description of the proposed NDA-MBE for MDS in MIMO frequency-selective channel is presented in Algorithm 3.

---

**Algorithm 3** : NDA-MBE for MDS in MIMO systems

---

- 1: Set  $f_l$ ,  $f_h$ ,  $\Delta$ , and  $\delta$
  - 2: Acquire the measurements  $\{r_k^{(n)}\}_{k=1}^N$ ,  $\forall n \in \{1, \dots, n_r\}$
  - 3: Estimate the statistics  $\hat{\mu}_2^{(n)}$ ,  $\hat{\mu}_4^{(n)}$ , and  $\hat{\kappa}_u^{(n)}$ , by employing (37) for  $\{r_k^{(n)}\}_{k=1}^N$ ,  $\forall n \in \{1, \dots, n_r\}$
  - 4: Compute  $\hat{\Psi}_u^{(n)}$ ,  $\forall u \in \{U_{\min}, \dots, U_{\max}\}$ ,  $\forall n \in \{1, \dots, n_r\}$ , by using (38)
  - 5: Compute  $\tilde{\Psi}_u$ ,  $\forall u \in \{U_{\min}, \dots, U_{\max}\}$ , by using (49)
  - 6: Obtain  $\hat{f}_D^{(r)}$  by solving the minimization problem in (40) for  $\tilde{\Psi}_u$  through the grid search method with step size  $\Delta$
  - 7: Obtain  $\hat{f}_D^{(s)}$  by solving the minimization problem in (40) for  $\tilde{\Psi}_u$  via the grid search method over  $[\hat{f}_D^{(r)} - \Delta, \hat{f}_D^{(r)} + \Delta]$  with step size  $\delta$
  - 8:  $\hat{f}_D = \hat{f}_D^{(s)}$
- 

Table I  
NUMBER OF REAL ADDITIONS, REAL MULTIPLICATIONS, AND COMPLEXITY ORDER OF THE PROPOSED NDA-MBE.

Algorithm	Real additions	Real multiplications	Order
MISO	$(N + 2N_g - \frac{(U_{\max} + U_{\min})}{2})N_{la} + 3N - N_g - 1$	$(N + N_g - \frac{(U_{\max} + U_{\min})}{2} + 2)N_{la} + 3N + 4$	$\mathcal{O}(N)$
MIMO	$n_r \left( (N - \frac{(U_{\max} + U_{\min})}{2})N_{la} + 3N - 1 \right) + (2N_{la} - 1)N_g$	$n_r \left( (N - \frac{(U_{\max} + U_{\min})}{2} + 2)N_{la} + 3N + 4 \right) + N_g N_{la} + 1$	$\mathcal{O}(N)$

### C. Semi-blind NDA-MBE

The proposed NDA-MBE for MISO and MIMO systems do not require knowledge of the parameter vector  $\varphi = [\beta^\dagger \xi^\dagger \boldsymbol{\theta}^\dagger f_D]^\dagger$ . In other words, the proposed NDA-MBE in section V-A and V-B are blind. For the scenarios in which the variance of the additive noise can be accurately estimated at the receive antennas, i.e.,  $\xi$  is known, a semi-blind NDA-MBE for the case of SISO transmission and flat-fading channel, i.e.,  $n_t = 1$  and  $L = 1$ , can be proposed. In this case, for the  $n$ th receive antennas, one can easily obtain<sup>6</sup>

$$\mu_2^{(n)} = \sigma_{h_n}^2 \sigma_s^2 + \sigma_{w_n}^2 \quad (50)$$

and

$$\eta^{(n)} = (\sigma_{h_n}^4 \sigma_s^4)^{-1} = \frac{1}{(\mu_2^{(n)} - \sigma_{w_n}^2)^2}. \quad (51)$$

By using (34), (50) and (51), and by replacing the statistical moments and the noise variance with their corresponding estimates, one obtains

$$\hat{\Psi}_u^{(n)} = \frac{\hat{\kappa}_u^{(n)} - \left(\hat{\mu}_2^{(n)}\right)^2}{\left(\hat{\mu}_2^{(n)} - \hat{\sigma}_w^2\right)^2}, \quad (52)$$

where  $\hat{\sigma}_{w_n}^2$  is the estimate of the noise variance, and  $\hat{\kappa}_u^{(n)}$  and  $\hat{\mu}_2^{(n)}$  are given in (37). Clearly, similar to the SISO transmission, the optimal and suboptimal combining methods for the multiple receive antennas can be employed, as well.

<sup>6</sup>The index of transmit antenna, i.e.,  $m = 1$  and the index of channel tap, i.e.,  $l = 1$  is dropped.

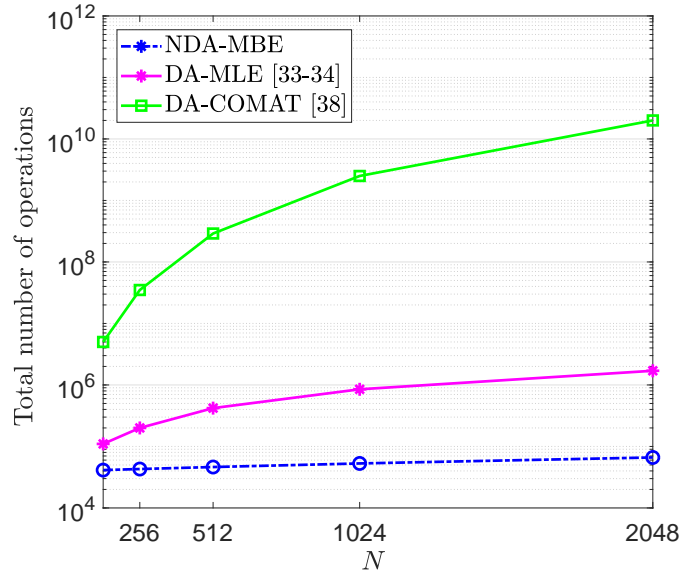


Fig. 2. Computational complexity comparison of the proposed NDA-MBE, the low-complexity DA-MLE in [33], [34], and the DA-COMAT estimator in [38].

## VI. COMPLEXITY ANALYSIS

By employing the two steps grid search method to solve the optimization problem in (40), the number of real additions and multiplications employed in the proposed NDA-MBE is shown in Table I, where  $N_{\text{la}}$  is the number of delay lag,  $N_{\text{g}} \triangleq (N_{\text{g}_1} + N_{\text{g}_2})$ , and  $N_{\text{g}_1}$  and  $N_{\text{g}_2}$  are the number of grid points used for the rough and fine estimation, respectively. As seen, the proposed NDA-MBE exhibits a complexity order of  $\mathcal{O}(N)$ . It should be mentioned that the complexity order of the derived DA-MLE and NDA-MLE are  $\mathcal{O}(N^3)$  and  $\mathcal{O}(|M|^{N' n_t})$ , respectively.

Fig. 2 compares the total number of operations used by the proposed NDA-MBE with the low-complexity DA-MLE in [33], [34] and the DA-COMAT estimator in [38]. As seen, the proposed NDA-MBE exhibits significantly lower computational complexity compared to the DA-COMAT [38] and the low-complexity DA-MLE in [33], [34]. This substantial reduced-complexity enables the proposed MBE to exhibit good performance in the NDA scenarios, where the observation window can be selected large enough.

## VII. SIMULATION RESULTS

In this section, we examine the performance of the proposed NDA-MBE, as well as the derived DA-MLE and DA-CRLB for MDS in MIMO frequency-selective fading channel through several simulation experiments.

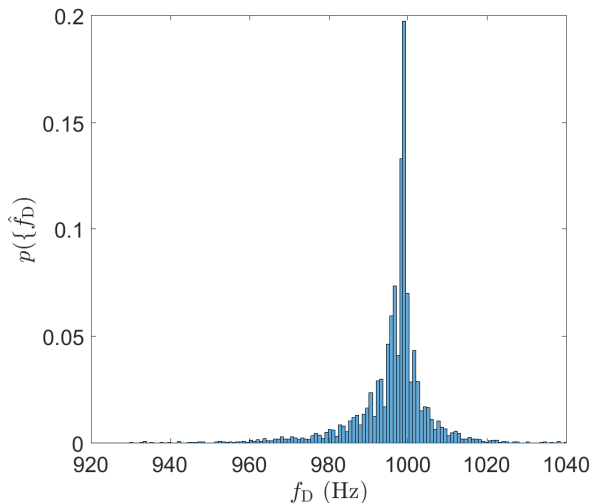
### A. Simulation Setup

We consider a MIMO system employing spatial multiplexing, with carrier frequency  $f_c = 2.4$  GHz. Unless otherwise mentioned,  $n_t = 2$ ,  $n_r = 2$ ,  $T_s = 10 \mu\text{s}$ ,  $N = 10^5$ , and the modulation is 64-QAM. The delay profile of the Rayleigh fading channel is  $\sigma_{h(mn),l}^2 = \beta \exp(-l_{\text{rms}} l / L)$ , where  $\beta$  is a normalization factor, i.e.,  $\beta \sum_l (-l_{\text{rms}} l / L) = 1$ , with  $L = 5$  and  $l_{\text{rms}} = L/4$  as the maximum and RMS delay spread of the channel, respectively. The parameters for the downsampled LS

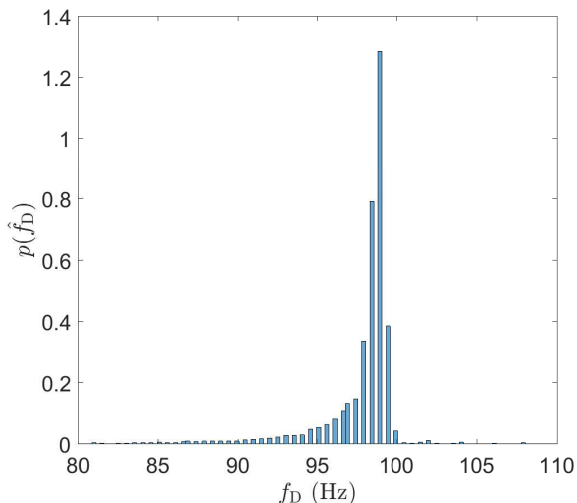
curve-fitting optimization are  $U_{\min} = L$ ,  $U_{\max} = \lfloor \frac{N}{10} \rfloor$ , and  $u_s = 10$ . The additive white noise was modeled as a complex-valued Gaussian random variable with zero-mean and variance  $\sigma_w^2$  for each receive antennas. Without loss of generality, it was assumed that  $\sigma_{s_m}^2 = 1/(n_t n_r)$ ,  $m = 1, 2, \dots, n_t$ , and thus, the average SNR was defined as  $\gamma = 10 \log(1/n_r \sigma_w^2)$ . Unless otherwise mentioned, the performance of the MDS estimators was presented in terms of normalized root-mean-square error (NRMSE), i.e.,  $\mathbb{E}\{(\hat{f}_D T_s - f_D T_s)^2\}^{1/2}/f_D T_s$ , obtained from 1000 Monte Carlo trials for each  $f_D T_s \in [10^{-3}, 18 \times 10^{-3}]$ , with the search step size  $\Delta = 10$  Hz and  $\delta = 0.5$  Hz, respectively.

### B. Simulation Results

Fig. 3 shows the distributions of the estimated  $\hat{f}_D$  by the proposed NDA-MBE for different MDSs,  $f_D = 1000$  Hz and  $f_D = 100$  Hz, with  $n_t = 2$ ,  $n_r = 2$ , and at  $\gamma = 10$  dB. As seen, the distributions are not symmetric around their mean values; hence, this leads to bias in MDS estimation. Furthermore, Fig. 4 illustrates  $\mathbb{E}\{\hat{f}_D/f_D\}$  versus  $f_D$  for  $\gamma = 10$  dB and  $\gamma = 20$  dB. As seen, the proposed NDA-MBE is nearly unbiased, i.e.,  $\mathbb{E}\{\hat{f}_D\} \approx f_D$  over a wide range of MDS. This can be



(a)  $f_D = 1000$  Hz



(b)  $f_D = 100$  Hz

Fig. 3. Distribution of the estimated  $\hat{f}_D$  for the proposed NDA-MBE for  $n_t = 2$ ,  $n_r = 2$ , and at  $\gamma = 10$  dB.

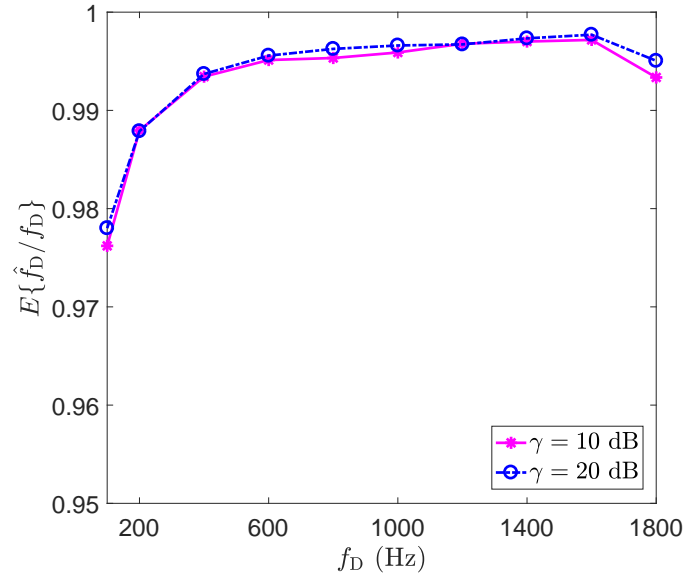


Fig. 4. The mean value of the estimated MDS by NDA-MBE for various SNR values for  $n_t = 2$  and  $n_r = 2$ .

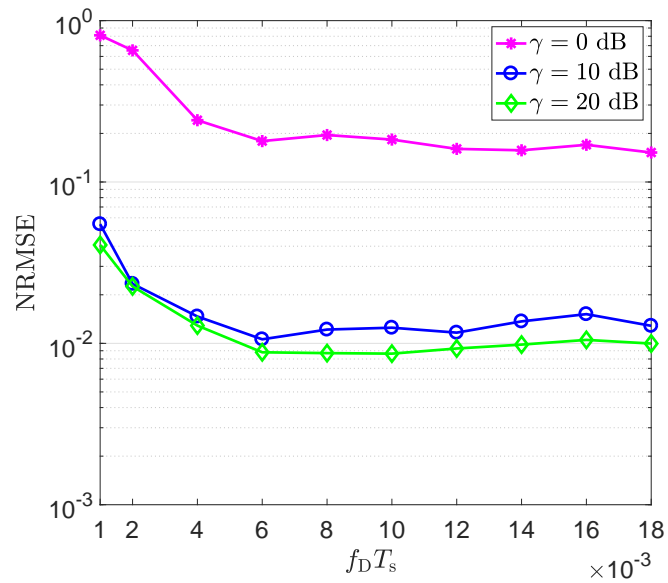


Fig. 5. The NRMSE of the proposed NDA-MBE versus  $f_D T_s$  for different SNR values.

explained, as while the distribution of the estimated  $f_D$  is not symmetric, the estimated values are accumulated around their mean value. It should be mentioned that by increasing the length of the observation window,  $N$ , the bias of the proposed estimator approaches zero.

In Fig. 5, the NRMSE of the NDA-MBE versus  $f_D T_s$  is illustrated for  $\gamma = 0$  dB,  $\gamma = 10$  dB, and  $\gamma = 20$  dB. As seen, the proposed estimator exhibits a good performance over a wide range of Doppler rates,  $f_D T_s$ . As observed, the NRMSE decreases as  $f_D T_s$  increases. This performance improvement can be explained, as for lower Doppler rates, a larger observation window

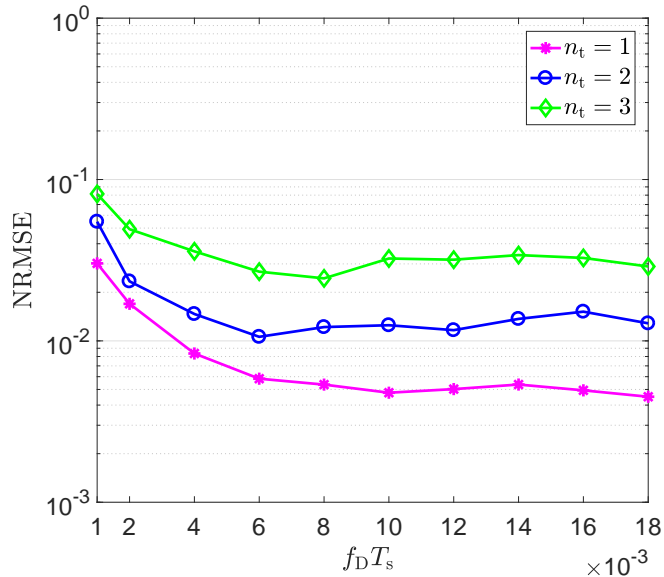


Fig. 6. The effect of  $n_t$  on the performance of the proposed NDA-MBE for  $n_r = 2$  and at  $\gamma = 10$  dB.

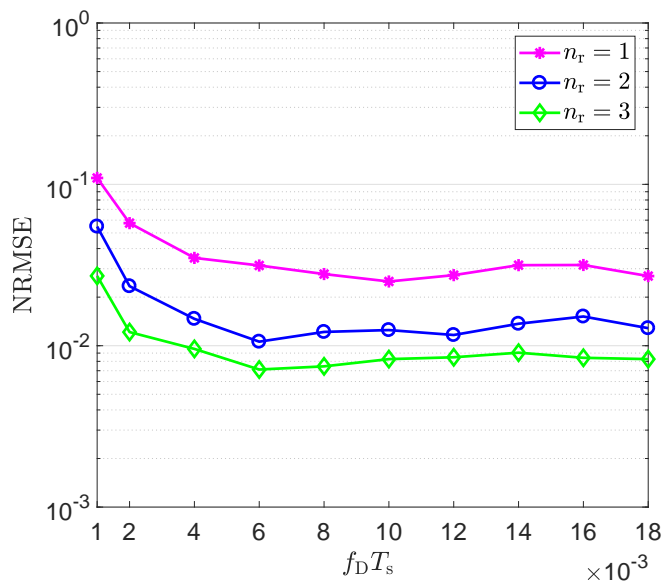


Fig. 7. The effect of  $n_r$  on the performance of the proposed NDA-MBE for  $n_t = 2$  and at  $\gamma = 10$  dB.

is required to capture the variation of the fading channel. Also, as expected, the NRMSE decreases as  $\gamma$  increases. This can be easily explained, as an increase in  $\gamma$  leads to more accurate estimates of the statistics in (38).

Fig. 6 presents the NRMSE of the proposed NDA-MBE versus  $f_D T_s$  for different numbers of transmit antennas,  $n_t$ , for  $n_r = 2$  and at  $\gamma = 10$  dB. As expected, the NRMSE increases as the number of transmit antennas increases. This increase can be explained, as the variance of the statistics employed in (38) increases with the number of transmit antennas, thus, leading to higher estimation error in the LS curve-fitting.

In Fig. 7, the NRMSE of the proposed NDA-MBE is shown versus  $f_D T_s$  for different numbers of receive antennas,  $n_r$ , for  $n_t = 2$ , and at  $\gamma = 10$  dB. It can be seen that an increment in  $n_r$  leads to a reduced NRMSE. This decrease can be easily

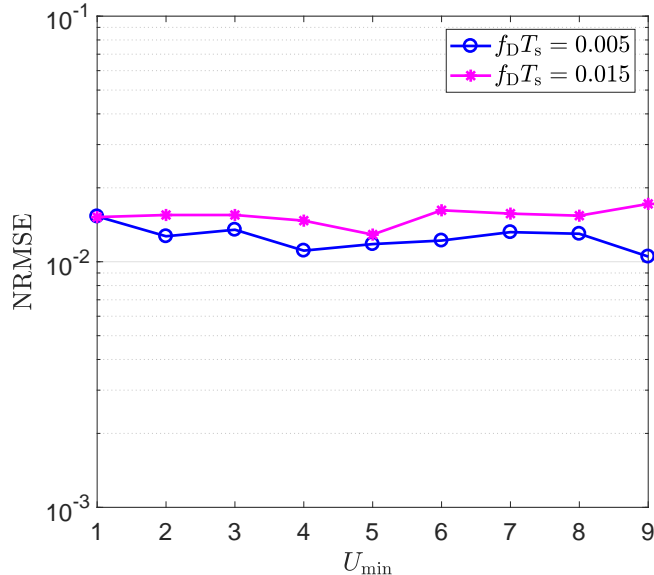


Fig. 8. The effect of the parameter  $U_{\min}$  on the performance of the proposed NDA-MBE for different values of  $f_d T_s$  and at  $\gamma = 10$  dB.

explained, as averaging at the receive-side yields more accurate estimation of  $\Psi_u$ , thus, leading to a more accurate result in the LS curve-fitting.

In Fig. 8, the effect of the parameter  $U_{\min}$  on the performance of the proposed NDA-MBE is illustrated for  $L = 5$  and  $u_s = 10$ . As observed, the proposed estimator exhibits a low sensitivity to the value of  $U_{\min}$ . This can be explained, as a large number of lags,  $U_{\min} \leq u \leq U_{\max}$ , are employed for fitting  $\tilde{\Psi}_u$  to  $J_0^2(2\pi f_D T_s u)$  in the LS estimation; thus, the estimator is nearly robust to a few missing delay lags,  $L \leq u < U_{\min}$ , or nuisance delay lags,  $1 \leq u < L$ . As such, basically the estimator does not require an accurate estimate of  $L$ .

Fig. 9 shows the effect of the observation window size,  $N$ , on the performance of the proposed NDA-MBE. As expected, the performance of the proposed estimator improves as the length of the observation window increases. This performance improvement can be explained, as the variance of the estimated statistics employed in (38) decreases when  $N$  increases.

In Fig. 10, the NRMSE is plotted versus  $f_d T_s$  for the proposed NDA-MBE, the low-complexity DA-MLE (DA-LMLE) in [33], [34], the NDA-CCE in [40], the DA-MLE in [30], and the DA-CRLB in [32] for MDS estimation in SISO frequency-flat fading channel for  $N = 1000$  and at  $\gamma = 10$  dB. As seen, the proposed NDA-MBE outperforms the NDA-CCE, and provides a similar performance as the DA-LMLE for  $f_d T_s \geq 0.012$ . The performance degradation of the DA-LMLE at high values of  $f_d T_s$  is related to the second-order Taylor expansion employed to approximate the covariance matrix; this is less accurate at higher MDSs.

Fig. 11 illustrates the NRMSE versus  $f_d T_s$  for the proposed NDA-MBE, the derived DA-MLE, and the derived DA-CRLB in MIMO frequency-selective fading channel for  $N = 1000$  and at  $\gamma = 10$  dB. In order to show the convergence problem in the derived DA-MLE caused by the Fisher-scoring numerical method employed to solve the ML [43], the performance of

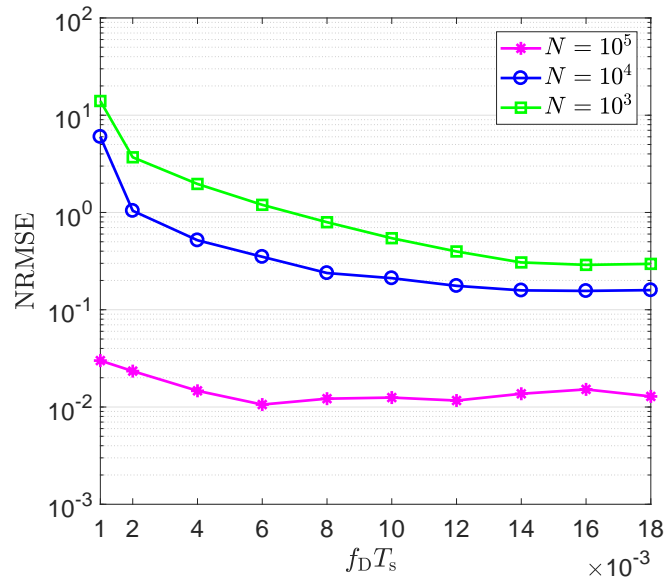


Fig. 9. The effect of the observation window size,  $N$ , on the performance of the proposed NDA-MBE for  $n_t = 2$  and  $n_r = 2$  in frequency-selective channel, and at  $\gamma = 10$  dB.

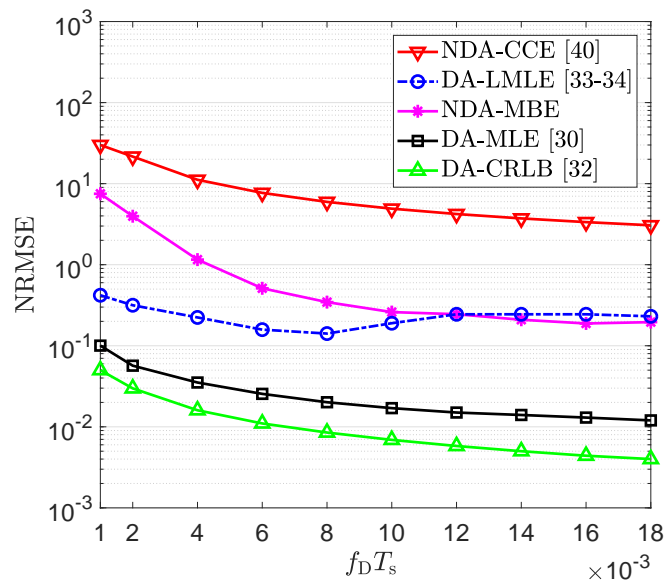


Fig. 10. Performance comparison of the proposed NDA-MBE, DA-CRLB [32], DA-MLE [30], the low-complexity DA-MLE in [33], [34], and the NDA-CCE in [40] in SISO frequency-flat fading channel for  $N = 10^3$  at  $\gamma = 10$  dB.

the derived DA-MLE for the cases of single initial value (SIV) and multiple initial values (MIV) is plotted, respectively.<sup>7</sup> As seen, by choosing MIV, the convergence problem of the Fisher-scoring method employed in the derived DA-MLE is solved. Moreover, as observed, the performance of the derived DA-MLE with MIV is close to the DA-CRLB. This high performance is obtained at the expense of significant computational complexity in the order of  $\mathcal{O}(N^3)$ . On the other hand, the proposed NDA-MBE cannot reach the DA-CRLB. This behaviour can be explained, as the NDA-MBE requires a larger number of observation symbols to accurately estimate the second- and fourth-order statistics in time-varying channel. However, the

<sup>7</sup>With the MIV method, several initial values are considered and at convergence the one that yields the maximum is chosen.

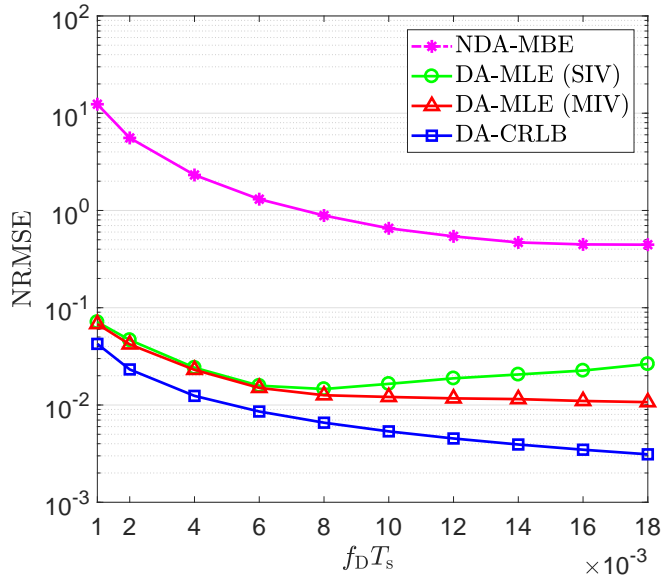


Fig. 11. Performance comparison of the proposed NDA-MBE, the derived DA-CRLB, and the derived DA-MLE (SIV and MIV) in MIMO frequency-selective Rayleigh fading channel for  $n_t = 2$ ,  $n_r = 2$ ,  $L = 5$ ,  $N = 10^3$ , and at  $\gamma = 10$  dB.

substantial reduced-complexity enables the proposed MBE to exhibit significantly low NRMSE in the NDA scenarios, where the observation window can be selected large enough.

In Fig. 12, the NRMSE is shown versus  $f_D T_s$  for the proposed semi-blind NDA-MBE in (52), the derived NDA-MLE, and the NDA-CRLB in SISO flat-fading channel for BPSK signal,  $N = 10$ ,  $f_D T_s \in [5 \times 10^{-3}, 45 \times 10^{-3}]$ , and at  $\gamma = 20$  dB.<sup>8</sup> As expected, the NDA-MBE does not exhibit good performance for a short observation window size because the second- and fourth-order statistics employed in (52) are not accurately estimated. On the other hand, the derived NDA-MLE exhibits low NRMSE even for a short observation window. Moreover, there is no significant performance gap between the derived NDA-MLE and NDA-CRLB, as well as the DA-MLE in [30] and the DA-CRLB in [32].

## VIII. CONCLUSION

In this paper, we derived the DA- and NDA-CRLBs and DA- and NDA-MLEs for MDS in MIMO frequency-selective fading channel. Moreover, a low-complexity NDA-MBE for MISO and MIMO systems was proposed. The NDA-MBE employs the statistical moment-based approach and relies on the second- and fourth-order statistics of the received signal, as well as the LS curve-fitting optimization technique. Compared to the existing DA estimators, the proposed NDA-MBE provides higher system capacity due to absence of pilot. Also, the substantial reduced-complexity enables the proposed MBE to exhibit good performance in the NDA scenarios, where the observation window can be selected large enough. The NDA-MBE does not require *a priori* knowledge of other parameters, such as the number of transmit antennas; furthermore, the proposed NDA-MBE is robust to the time-frequency asynchronization. When compared to the NDA-CCE, the NDA-MBE exhibits better

<sup>8</sup>The complexity order of the derived NDA-MLE and NDA-CRLB are in the order of  $\mathcal{O}(|M|^{N' n_t})$ ; for large values of  $N'$  ( $N' = N + L - 1$ ), the corresponding curves are not obtainable even for  $|M| = 2$  or  $n_t = 1$ . Hence,  $N = 10$  and SISO flat-fading channel are considered.

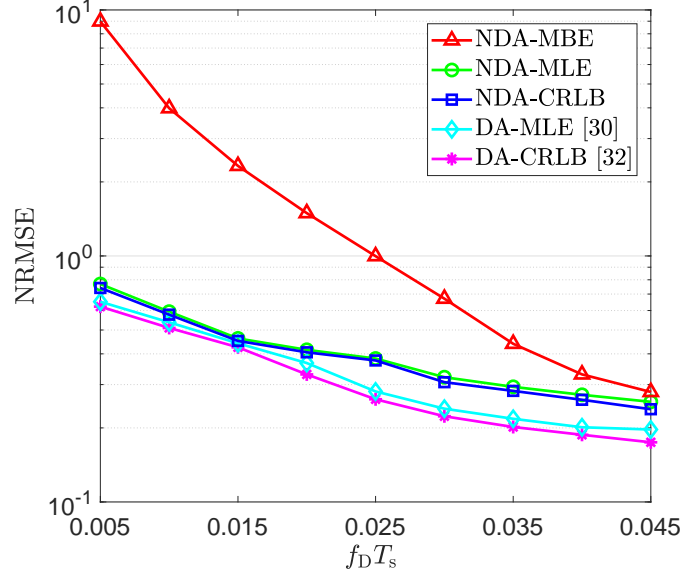


Fig. 12. Performance comparison of the proposed semi-blind NDA-MBE in (52), the derived NDA-MLE, the derived NDA-CRLB, the DA-MLE in [30], and the DA-CRLB in [32] in SISO frequency-flat-fading channel for  $N = 10$  and at  $\gamma = 20$  dB SNR.

$$\begin{aligned}
|r_k^{(n)}|^2 &= \sum_{m=1}^{n_t} \sum_{l=1}^L |h_{k,l}^{(mn)}|^2 |s_{k-l}^{(m)}|^2 + \sum_{m_1=1}^{n_t} \sum_{m_2 \neq m_1}^{n_t} \sum_{l=1}^L h_{k,l}^{(m_1 n)} (h_{k,l}^{(m_2 n)})^* s_{k-l}^{(m_1)} (s_{k-l}^{(m_2)})^* \\
&+ \sum_{m=1}^{n_t} \sum_{l_1=1}^L \sum_{l_2 \neq l_1}^L h_{k,l_1}^{(mn)} (h_{k,l_2}^{(mn)})^* s_{k-l_1}^{(m)} (s_{k-l_2}^{(m)})^* + \sum_{m_1=1}^{n_t} \sum_{m_2 \neq m_1}^{n_t} \sum_{l_1=1}^L \sum_{l_2 \neq l_1}^L h_{k,l_1}^{(m_1 n)} (h_{k,l_2}^{(m_2 n)})^* s_{k-l_1}^{(m_1)} (s_{k-l_2}^{(m_2)})^* \\
&+ (w_k^{(n)})^* \sum_{m=1}^{n_t} \sum_{l=1}^L h_{k,l}^{(mn)} s_{k-l}^{(m)} + (w_k^{(n)}) \sum_{m=1}^{n_t} \sum_{l=1}^L (h_{k,l}^{(mn)})^* (s_{k-l}^{(m)})^* + |w_k^{(n)}|^2.
\end{aligned} \tag{53}$$

$$\begin{aligned}
\kappa_u^{(n)} &= \sum_{m=1}^{n_t} \sum_{l=1}^L \mathbb{E} \left\{ |h_{k,l}^{(mn)}|^2 |h_{k+u,l}^{(mn)}|^2 \right\} \mathbb{E} \left\{ |s_{k-l}^{(m)}|^2 |s_{k+u-l}^{(m)}|^2 \right\} + \sum_{m_1=1}^{n_t} \sum_{m_2 \neq m_1}^{n_t} \sum_{l=1}^L \mathbb{E} \left\{ |h_{k,l}^{(m_1 n)}|^2 |h_{k+u,l}^{(m_2 n)}|^2 \right\} \mathbb{E} \left\{ |s_{k-l}^{(m_1)}|^2 |s_{k+u-l}^{(m_2)}|^2 \right\} \\
&+ \sum_{m=1}^{n_t} \sum_{l_1=1}^L \sum_{l_2 \neq l_1}^L \mathbb{E} \left\{ |h_{k,l_1}^{(mn)}|^2 |h_{k+u,l_2}^{(mn)}|^2 \right\} \mathbb{E} \left\{ |s_{k-l_1}^{(m)}|^2 |s_{k+u-l_2}^{(m)}|^2 \right\} \\
&+ \sum_{m_1=1}^{n_t} \sum_{m_2 \neq m_1}^{n_t} \sum_{l_1=1}^L \sum_{l_2 \neq l_1}^L \mathbb{E} \left\{ |h_{k,l_1}^{(m_1 n)}|^2 |h_{k+u,l_2}^{(m_2 n)}|^2 \right\} \mathbb{E} \left\{ |s_{k-l_1}^{(m_1)}|^2 |s_{k+u-l_2}^{(m_2)}|^2 \right\} + \mathbb{E} \left\{ |w_{k+u}^{(n)}|^2 \right\} \sum_{m=1}^{n_t} \sum_{l=1}^L \mathbb{E} \left\{ |h_{k,l}^{(mn)}|^2 \right\} \mathbb{E} \left\{ |s_{k-l}^{(m)}|^2 \right\} \\
&+ \mathbb{E} \left\{ |w_k^{(n)}|^2 \right\} \sum_{m=1}^{n_t} \sum_{l=1}^L \mathbb{E} \left\{ |h_{k+u,l}^{(mn)}|^2 \right\} \mathbb{E} \left\{ |s_{k+u-l}^{(m)}|^2 \right\} + \mathbb{E} \left\{ |w_k^{(n)}|^2 \right\} \mathbb{E} \left\{ |w_{k+u}^{(n)}|^2 \right\}.
\end{aligned} \tag{54}$$

performance, and when compared to the low-complexity DA-MLE, it exhibits similar performance for high MDSs. On the other hand, the derived DA-MLE's performance is very close to the derived DA-CRLB in MIMO frequency-selective channel even when the observation window is relatively small. Similarly, there is no significant performance gap between the derived NDA-MLE and the NDA-CRLB.

## APPENDIX I

To obtain an explicit closed-form expression for  $\kappa_u^{(n)} \triangleq \mathbb{E}\{|r_k^{(n)}|^2 |r_{k+u}^{(n)}|^2\}$ , we first write  $|r_k^{(n)}|^2 = r_k^{(n)} (r_k^{(n)})^*$  by employing (1), as in (53) at the top of next page. Then,  $|r_{k+u}^{(n)}|^2$  is straightforwardly calculated by replacing  $k$  with  $k+u$  in (53), and  $|r_k^{(n)}|^2 |r_{k+u}^{(n)}|^2$  can be easily expressed in a summation form, which is omitted due to space constraints.

As fading is independent of the signal and noise, the statistical expectation in  $\kappa_u^{(n)}$  can be decomposed into statistical expectations over the signal, fading, and noise distributions, respectively. With independent and identically distributed transmitted symbols,  $s_k^{(m)}$ ,  $k = 1, \dots, N$ , and  $u \geq L$ , the symbols from the  $m$ th antenna contributed in  $r_k^{(n)}$ , i.e.,  $\{s_{k-l}^{(m)}\}_{l=1}^L$ , are different from those contributed in  $r_{k+u}^{(n)}$ , i.e.,  $\{s_{k+u-l}^{(m)}\}_{l=1}^L$ ; furthermore, by using that  $\mathbb{E}\{(s_k^{(m)})^2\} = 0$ ,  $\mathbb{E}\{s_k^{(m)}\} = 0$ , and the linearity property of the statistical expectation, one obtains  $\kappa_u^{(n)}$  as in (54). Finally, with  $\mathbb{E}\{|s_k^{(m)}|^2\} = \sigma_{s_m}^2$  and  $\mathbb{E}\{|w_k^{(n)}|^2\} = \sigma_{w_n}^2$ , (28) is obtained.  $\square$

## APPENDIX II

By employing (33), one can write

$$\begin{aligned}
(\mu_2^{(n)})^2 &= \left( \sum_{m=1}^{n_t} \sum_{l=1}^L \sigma_{h(mn),l}^2 \sigma_{s_m}^2 + \sigma_{w_n}^2 \right)^2 = \sum_{m=1}^{n_t} \sum_{l=1}^L \sigma_{h(mn),l}^4 \sigma_{s_m}^4 \\
&+ \sum_{m_1=1}^{n_t} \sum_{m_2 \neq m_1}^{n_t} \sum_{l=1}^L \sigma_{h(m_1 n),l}^2 \sigma_{h(m_2 n),l}^2 \sigma_{s_{m_1}}^2 \sigma_{s_{m_2}}^2 \\
&+ \sum_{m=1}^{n_t} \sum_{l_1=1}^L \sum_{l_2 \neq l_1}^L \sigma_{h(mn),l_1}^2 \sigma_{h(mn),l_2}^2 \sigma_{s_m}^4 \\
&+ \sum_{m_1=1}^{n_t} \sum_{m_2 \neq m_1}^{n_t} \sum_{l_1=1}^L \sum_{l_2 \neq l_1}^L \sigma_{h(m_1 n),l_1}^2 \sigma_{h(m_2 n),l_2}^2 \sigma_{s_{m_1}}^2 \sigma_{s_{m_2}}^2 \\
&+ 2\sigma_{w_n}^2 \sum_{m=1}^{n_t} \sum_{l=1}^L \sigma_{h(mn),l}^2 \sigma_{s_m}^2 + \sigma_{w_n}^4.
\end{aligned} \tag{55}$$

Then, by subtracting  $(\mu_2^{(n)})^2$  in (55) from  $\kappa_u^{(n)}$  in (32), one obtains

$$\kappa_u^{(n)} - (\mu_2^{(n)})^2 = \frac{J_0^2(2\pi f_D T_s u)}{\eta^{(n)}}, \tag{56}$$

where  $\eta^{(n)} = 1 / \sum_{m=1}^{n_t} \sum_{l=1}^L \sigma_{h(mn),l}^4 \sigma_{s_m}^4$ .

## APPENDIX III

With independent fading, noise, and signal processes, by using (53) and then (31) and that  $\mathbb{E}\{(s_k^{(m)})^2\} = \mathbb{E}\{s_k^{(m)}\} = \mathbb{E}\{(h_{k,l}^{(mn)})^2\} = \mathbb{E}\{w_k^{(n)}\} = 0$ , similar to Appendix I, one obtains

$$\begin{aligned}
\mu_4^{(n)} &= \mathbb{E}\{|r_k^{(n)}|^4\} = 2 \sum_{m=1}^{n_t} \sum_{l=1}^L \sigma_{h(mn),l}^4 \sigma_{s_m}^4 \\
&+ 2 \sum_{m=1}^{n_t} \sum_{l=1}^L \sigma_{h(mn),l}^4 (\Omega_s - 1) \sigma_{s_m}^4
\end{aligned} \tag{57}$$

$$\begin{aligned}
& + 2 \sum_{m_1=1}^{n_t} \sum_{m_2 \neq m_1}^{n_t} \sum_{l=1}^L \sigma_{h(m_1 n), l}^2 \sigma_{h(m_2 n), l}^2 \sigma_{s_{m_1}}^2 \sigma_{s_{m_2}}^2 \\
& + 2 \sum_{m=1}^{n_t} \sum_{l_1=1}^L \sum_{l_2 \neq l_1}^L \sigma_{h(m n), l_1}^2 \sigma_{h(m n), l_2}^2 \sigma_{s_m}^4 \\
& + 2 \sum_{m_1=1}^{n_t} \sum_{m_2 \neq m_1}^{n_t} \sum_{l_1=1}^L \sum_{l_2 \neq l_1}^L \sigma_{h(m_1 n), l_1}^2 \sigma_{h(m_2 n), l_2}^2 \sigma_{s_{m_1}}^2 \sigma_{s_{m_2}}^2 \\
& + 4\sigma_{w_n}^2 \sum_{m=1}^{n_t} \sum_{l=1}^L \sigma_{h(m n), l}^2 \sigma_{s_m}^2 + 2\sigma_{w_n}^4,
\end{aligned}$$

where  $\Omega_s$  is the fourth-order two-conjugate statistic for unit variance signal, which represents the effect of the modulation format. Finally, by employing (33) and (57), (35) is easily obtained.  $\square$

## REFERENCES

- [1] A. F. Molisch, *Wireless Communications*. John Wiley & Sons, 2007.
- [2] G. L. Stüber, *Principles of Mobile Communication*. Springer Science & Business Media, 2011.
- [3] J. Wu and P. Fan, "A survey on high mobility wireless communications: Challenges, opportunities and solutions," *IEEE Access*, vol. 4, pp. 450–476, Jan. 2016.
- [4] M. J. Chu and W. E. Stark, "Effect of mobile velocity on communications in fading channels," *IEEE Trans. Veh. Technol.*, vol. 49, no. 1, pp. 202–210, Jan. 2000.
- [5] A. J. Goldsmith and S.-G. Chua, "Variable-rate variable-power M-QAM for fading channels," *IEEE Trans. Commun.*, vol. 45, no. 10, pp. 1218–1230, Oct. 1997.
- [6] K. Balachandran, S. R. Kadaba, and S. Nanda, "Channel quality estimation and rate adaptation for cellular mobile radio," *IEEE J. Sel. Areas Commun.*, vol. 17, no. 7, pp. 1244–1256, July 1999.
- [7] C. Tepedelenliođlu, A. Abdi, G. B. Giannakis, and M. Kaveh, "Estimation of Doppler spread and signal strength in mobile communications with applications to handoff and adaptive transmission," *Wirel. Commun. Mob. Comput.*, vol. 1, no. 2, pp. 221–242, Mar. 2001.
- [8] M. D. Austin and G. L. Stüber, "Velocity adaptive handoff algorithms for microcellular systems," *IEEE Trans. Veh. Technol.*, vol. 43, no. 3, pp. 549–561, Aug. 1994.
- [9] B. L. Mark and A. E. Leu, "Local averaging for fast handoffs in cellular networks," *IEEE Trans. Wireless Commun.*, vol. 6, no. 3, pp. 866–874, Mar. 2007.
- [10] A. Duel-Hallen, S. Hu, and H. Hallen, "Long-range prediction of fading signals," *IEEE Signal Process. Mag.*, vol. 17, no. 3, pp. 62–75, May 2000.
- [11] D.-S. Shiu, G. J. Foschini, M. J. Gans, and J. M. Kahn, "Fading correlation and its effect on the capacity of multi-element antenna systems," *IEEE Trans. Commun.*, vol. 48, no. 3, pp. 502–513, Mar. 2000.
- [12] C.-N. Chuah *et al.*, "Capacity scaling in MIMO wireless systems under correlated fading," *IEEE Trans. Inf. Theory*, vol. 48, no. 3, pp. 637–650, Mar. 2002.
- [13] T. Yucek, R. Tannious, and H. Arslan, "Doppler spread estimation for wireless OFDM systems," in *Proc. IEEE Advances in Wired and Wireless Communication*, Princeton, USA, Apr. 2005, pp. 233–236.
- [14] S. Coleri, M. Ergen, A. Puri, and A. Bahai, "Channel estimation techniques based on pilot arrangement in OFDM systems," *IEEE Trans. Broadcast.*, vol. 48, no. 3, pp. 223–229, Sept. 2002.
- [15] F. Bellili, R. Meftehi, S. Affes, and A. Stéphenne, "Maximum likelihood SNR estimation of linearly-modulated signals over time-varying flat-fading SIMO channels," *IEEE Trans. Signal Process.*, vol. 63, no. 2, pp. 441–456, Jan. 2015.
- [16] M. Marey, M. Samir, and O. A. Dobre, "EM-based joint channel estimation and IQ imbalances for OFDM systems," *IEEE Trans. Broadcast.*, vol. 58, no. 1, pp. 106–113, Mar. 2012.
- [17] A. Khansefid and H. Minn, "On channel estimation for massive MIMO with pilot contamination," *IEEE Commun. Lett.*, vol. 19, no. 9, pp. 1660–1663, Sept. 2015.

- [18] Y. Li, H. Minn, and M. Z. Win, "Frequency offset estimation for MB-OFDM-based UWB systems," *IEEE Trans. Commun.*, vol. 56, no. 6, pp. 968–979, Jun. 2008.
- [19] M. Mohammadkarimi, O. A. Dobre, and M. Z. Win, "Non-Data-Aided SNR Estimation for Multiple Antenna Systems," in *Proc. GLOBECOM*, Washington, USA, Dec. 2016, pp. 1–5.
- [20] H. Wang, O. A. Dobre, C. Li, and D. C. Popescu, "Blind cyclostationarity-based symbol period estimation for FSK signals," *IEEE Commun. Lett.*, vol. 19, no. 7, pp. 1149–1152, July 2015.
- [21] A. Masmoudi, F. Bellili, S. Affes, and A. Stephenne, "A non-data-aided maximum likelihood time delay estimator using importance sampling," *IEEE Trans. Signal Process.*, vol. 59, no. 10, pp. 4505–4515, Oct. 2011.
- [22] M. Mohammadkarimi, E. Karami, O. A. Dobre, and M. Z. Win, "Number of transmit antennas detection using time-diversity of the fading channel," *IEEE Trans. Signal Process.*, vol. 65, no. 15, pp. 4031–4046, Aug. 2017.
- [23] A. Stéphenne, F. Bellili, and S. Affes, "Moment-based SNR estimation over linearly-modulated wireless SIMO channels," *IEEE Trans. Wireless Commun.*, vol. 9, no. 2, pp. 714–722, Feb. 2010.
- [24] F. Bellili, A. Methenni, S. B. Amor, S. Affes, and A. Stéphenne, "Time synchronization of turbo-coded square-QAM-modulated transmissions: code-aided ML estimator and closed-form Cramér-Rao lower bounds," *IEEE Trans. Veh. Technol.*, vol. PP, no. 91, pp. 1–1, 2017.
- [25] F. Bellili, A. Methenni, and S. Affes, "Closed-form CRLBs for SNR estimation from turbo-coded BPSK-, MSK-, and square-QAM-modulated signals," *IEEE Trans. Signal Process.*, vol. 62, no. 15, pp. 4018–4033, Aug. 2014.
- [26] N. Wu, H. Wang, J. Kuang, and C. Yan, "Performance analysis of code-aided symbol timing recovery on AWGN channels," *IEEE Trans. Commun.*, vol. 59, no. 7, pp. 1975–1984, Mar. 2011.
- [27] C. Herzet, N. Noels, V. Lottici, H. Wymeersch, M. Luise, M. Moeneclaey, and L. Vandendorpe, "Code-aided turbo synchronization," *Proc. IEEE*, vol. 95, no. 6, pp. 1255–1271, July 2007.
- [28] F. Simoons and M. Moeneclaey, "Reduced complexity data-aided and code-aided frequency offset estimation for flat-fading MIMO channels," vol. 5, no. 6, pp. 1558–1567, Jun 2006.
- [29] J. Sun and M. C. Valenti, "Joint synchronization and SNR estimation for turbo codes in AWGN channels," *IEEE Trans. Commun.*, vol. 53, no. 7, pp. 1136–1144, July 2005.
- [30] L. Krasny, H. Arslan, D. Koilpillai, and S. Chennakeshu, "Doppler spread estimation in mobile radio systems," *IEEE Commun. Lett.*, vol. 5, no. 5, pp. 197–199, May 2001.
- [31] Y.-R. Tsai and K.-J. Yang, "Approximate ML Doppler spread estimation over flat Rayleigh fading channels," *IEEE Signal Process. Lett.*, vol. 16, no. 11, pp. 1007–1010, Nov. 2009.
- [32] A. Dogandžić and B. Zhang, "Estimating Jakes' Doppler power spectrum parameters using the Whittle approximation," *IEEE Trans. Signal Process.*, vol. 53, no. 3, pp. 987–1005, Mar. 2005.
- [33] F. Bellili, Y. Selmi, S. Affes, and A. Ghayeb, "A low-cost and robust maximum likelihood joint estimator for the Doppler spread and CFO parameters over flat-fading Rayleigh channels," *IEEE Trans. Commun.*, pp. 1–1, 2017.
- [34] F. Bellili and S. Affes, "A low-cost and robust maximum likelihood Doppler spread estimator," in *Proc. GLOBECOM*, Atlanta, USA, Dec. 2013, pp. 4325–4330.
- [35] K. E. Baddour and N. C. Beaulieu, "Nonparametric Doppler spread estimation for flat fading channels," in *Proc. WCNC*, New Orleans, USA, 2003, pp. 953–958.
- [36] K. D. Anim-Appiah, "On generalized covariance-based velocity estimation," *IEEE Trans. Veh. Technol.*, vol. 48, no. 5, pp. 1546–1557, Sept. 1999.
- [37] A. Abdi, H. Zhang, and C. Tepedelenlioglu, "A unified approach to the performance analysis of speed estimation techniques in mobile communication," *IEEE Trans. Wireless Commun.*, vol. 56, no. 1, pp. 126–135, Jan. 2008.
- [38] M. Souden, S. Affes, J. Benesty, and R. Bahroun, "Robust Doppler spread estimation in the presence of a residual carrier frequency offset," *IEEE Trans. Signal Process.*, vol. 57, no. 10, pp. 4148–4153, Oct. 2009.
- [39] G. Park, D. Hong, and C. Kang, "Level crossing rate estimation with Doppler adaptive noise suppression technique in frequency domain," in *Proc. IEEE VTC*, Orlando, USA, Oct. 2003, pp. 1192–1195.
- [40] H. Zhang and A. Abdi, "Cyclostationarity-based Doppler spread estimation in mobile fading channels," *IEEE Trans. Commun.*, vol. 57, no. 4, pp. 1061–1067, Apr. 2009.

- [41] E. Biglieri, R. Calderbank, A. Constantinides, A. Goldsmith, A. Paulraj, and H. V. Poor, *MIMO Wireless Communications*. Cambridge University press, 2007.
- [42] N. T. Longford, "A fast scoring algorithm for maximum likelihood estimation in unbalanced mixed models with nested random effects," *Biometrika*, vol. 74, no. 4, pp. 817–827, 1987.
- [43] S. M. Kay, *Fundamentals of Statistical Signal Processing, Vol. I: Estimation Theory*. Prentice Hall, 1993.
- [44] A. Swami and B. M. Sadler, "Hierarchical digital modulation classification using cumulants," *IEEE Trans. Commun.*, vol. 48, no. 3, pp. 416–429, Mar. 2000.
- [45] K. E. Baddour and N. C. Beaulieu, "Autoregressive modeling for fading channel simulation," *IEEE Trans. Wireless Commun.*, vol. 4, no. 4, pp. 1650–1662, July 2005.
- [46] P. Sadeghi, R. A. Kennedy, P. B. Rapajic, and R. Shams, "Finite-state Markov modeling of fading channels-a survey of principles and applications," *IEEE Signal Process. Mag.*, vol. 25, no. 5, pp. 57–80, Sept. 2008.
- [47] I. Reed, "On a moment theorem for complex Gaussian processes," *IEEE Trans. Inf. Theory*, vol. 3, no. 8, pp. 194–195, Apr. 1962.
- [48] A. R. Gallant, *Nonlinear Statistical Models*. John Wiley & Sons, 2009, vol. 310.
- [49] N. R. Draper, H. Smith, and E. Pownell, *Applied Regression Analysis*. Wiley New York, 1966, vol. 3.
- [50] S. S. Rao and S. Rao, *Engineering Optimization: Theory and Practice*. John Wiley & Sons, 2009.
- [51] A. M. Zoubir and B. Boashash, "The bootstrap and its application in signal processing," *IEEE Signal Process. Mag.*, vol. 15, no. 1, pp. 56–76, Jan. 1998.
- [52] A. M. Zoubir and D. R. Iskander, "Bootstrap methods and applications," *IEEE Signal Process. Mag.*, vol. 24, no. 4, pp. 10–19, July 2007.
- [53] A. M. Zoubir and D. R. Iskander, "Bootstrap modeling of a class of nonstationary signals," *IEEE Trans. Signal Process.*, vol. 48, no. 2, pp. 399–408, Feb. 2000.